Overcoming Sparsity Artifacts in Crosscoders to Interpret Chat-Tuning

Anonymous Author(s)
Affiliation
Address
email

Abstract

Model diffing is the study of how fine-tuning changes a model's representations and internal algorithms. Many behaviors of interest are introduced during fine-tuning, and model diffing offers a promising lens to interpret such behaviors. Crosscoders are a recent model diffing method that learns a shared dictionary of interpretable concepts represented as latent directions in both the base and fine-tuned models, allowing us to track how concepts shift or emerge during fine-tuning. Notably, prior work has observed concepts with no direction in the base model, and it was hypothesized that these model-specific latents were concepts introduced during fine-tuning. However, we identify two issues which stem from the crosscoders L1 training loss that can misattribute concepts as unique to the fine-tuned model, when they really exist in both models. We develop Latent Scaling to flag these issues by more accurately measuring each latent's presence across models. In experiments comparing Gemma 2 2B base and chat models, we observe that the standard crosscoder suffers heavily from these issues. Building on these insights, we train a crosscoder with BatchTopK loss and show that it substantially mitigates these issues, finding more genuinely chat-specific and highly interpretable concepts. We recommend practitioners adopt similar techniques. Using the BatchTopK crosscoder, we successfully identify a set of chat-specific latents that are both interpretable and causally effective, representing concepts such as *false information* and *personal question*, along with multiple refusal-related latents that show nuanced preferences for different refusal triggers. Overall, our work advances best practices for the crosscoder-based methodology for model diffing and demonstrates that it can provide concrete insights into how chat-tuning modifies model behavior. [1]

1 Introduction

Classically, mechanistic interpretability [1, 2, 3, 4, 5] aims to reverse engineer an entire model [6, 7], or *circuits* implemented by the model to solve particular tasks [8]. *Model diffing* offers an alternative method by focusing on *changes* induced by fine-tuning. Since fine-tuning typically involves far less compute than the pre-training phase that establishes general knowledge and generic circuitry, its resulting modifications are expected to be limited in scope. This targeted nature suggests model diffing could be a *more tractable* approach to mechanistic interpretability than the full model analysis, while still providing valuable insights into core features of a model's behavior.

Model diffing might indeed be incredibly useful. The process of fine-tuning a model is what makes it *useful* as a tool or agent. Better understanding the mechanisms that give reasoning models [9, 10]

[1] We will release our code, crosscoder training library, models, training runs, and a demo notebook to explore latents after deanonymization.

Submitted to 39th Conference on Neural Information Processing Systems (NeurIPS 2025). Do not distribute.

heightened capabilities as compared to base or chat models might allow us to debug their failures and improve them. Fine-tuning also often introduces a number of problematic behaviors, for example, sycophancy [11]. Future AI safety and alignment concerns [12, 13, 14] may emerge specifically in fine-tuned models. For example, long-horizon RL could incentivize models to exploit reward signals and act deceptively. Model diffing could allow us to detect this.

Prior model diffing research has investigated how models change during fine-tuning [15, 16, 17, 18, 19, 20, 21, 22, 23, 24, 25, 26, 27, 28, 29]. While these studies have hypothesized that fine-tuning primarily shifts and repurposes existing capabilities rather than developing new ones, conclusive evidence for this claim remains elusive. Model diffing remains a nascent field that lacks established consensus and mature analytical tools. Much prior work has leveraged ad-hoc techniques for understanding how models change in narrow ways (e.g. focusing on a particular circuit), or have been on toy model. It is unclear whether prior approaches would scale to understanding the kinds of fine-tuning large models actually undergo.

Recently, Lindsey et al. [16] introduced the **crosscoder**, a novel and scalable tool for model diffing. Crosscoders build on the popular sparse autoencoder (SAE) [6, 30, 31], which has shown promise for interpreting a model's representations by decomposing activations into a sum of sparsely activating dictionary elements. There are many variants of crosscoders; the variant we are concerned with in this paper concatenates the activations of the base and chat-tuned model residual streams and trains a shared dictionary across this activation stack. Thus, for each dictionary element (aka "latent", corresponding to one concept), the crosscoder learns a pair of latent directions - one corresponding to the base model and one to the chat-tuned model. Crosscoders can thus potentially identify which latents are novel to the fine-tuned model, which are novel to the base-model, and which are shared. We term these sets chat-only, base-only, and shared respectively. Lindsey et al. [16] identify chat-only latents by looking at the norm of the latent directions – if the latent direction of the base model has zero norm, this indicates that the latent is chat-only.

In this work, we critically examine the crosscoder and identify two theoretical limitations of its training objective, that may lead to falsely identified chat-only latents (Section 2.2):

1. Complete Shrinkage: The sparsity loss can force base latent directions to zero norm, even when they contribute to base model reconstruction.
2. Latent Decoupling: The crosscoder may represent a shared concept using a chat-only latent when it is actually encoded by a different combination of latents in the base model, as the crosscoder's sparsity loss treats both representations as equivalent.

We develop an approach called *Latent Scaling* to detect spurious chat-only latents, inspired by Wright and Sharkey's [32] SAE scaling (Section 2.3), and demonstrate that the above issues occur in practice. While the norm-based metric from Lindsey et al. [16] appears to identify a clean trimodal distribution of base-only, shared and chat-only latents, we show that this is an artifact of the loss function rather than a meaningful distinction. Our conclusion is that the crosscoder loss does not actually have an inductive bias that helps to learn better model-only latents. Nonetheless, we demonstrate that crosscoders trained with BatchTopK loss [33] exhibit robustness to the above issues (Section 3.1) and identify a larger number of genuine model-specific latents. We show that in the BatchTopK crosscoder, the norm-based metric successfully identifies causally relevant latents by measuring their ability to reduce the prediction gap between base and chat model. In contrast, this metric fails in the L1 crosscoder, where Latent Scaling becomes necessary to identify the truly causally relevant latents. Finally, we outline that the chat-only latents found by the BatchTopK crosscoder are highly interpretable (Section 3.3), revealing key aspects of chat model behavior such as the role of chat template tokens, persona-related questions, detection of false information, and various refusal related mechanisms.

Overall, we show that using BatchTopK loss overcomes the described limitations of L1-trained crosscoders, validating them as a useful tool for understanding fine-tuning effects in large language models.

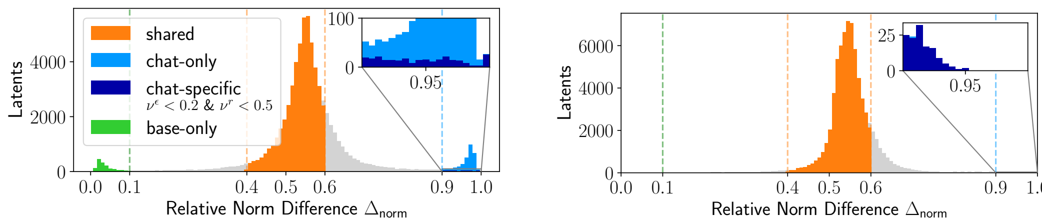

(a) L1 crosscoder.

(b) BatchTopK crosscoder.

Figure 1: Histogram of decoder latent relative norm differences (Δ_{norm}) between base and chat Gemma 2 2B models [34], for both the L1 crosscoder (left) and the BatchTopK crosscoder (right). A value of 1 means the decoder vector of a latent for the base model is zero, indicating the latent is not useful for the base model (*chat-only* latents). A value of 0 means the chat model's decoder vector has a norm of zero (*base-only* latents). Values around 0.5 indicate similar decoder norms in both models, suggesting equal utility in both models (*shared* latents)[3]. We also show the *chat-only* latents that are truly chat-specific and that are not affected by Complete Shrinkage (error ratio $\nu^{\varepsilon} < 0.2$) and Latent Decoupling (reconstruction ratio $\nu^{r} < 0.5$) – the *chat-specific* latents. Most of the L1 crosscoder *chat-only* latents suffer from these issues.

2 Methods

2.1 Crosscoder architectures

To build intuition, the crosscoder's goal is to learn a dictionary of interpretable concepts (latents) that can explain the activations of both models. It consists of an encoder and a decoder. The encoder takes the activations of the base and chat models and projects them into a shared high-dimensional sparse space, where each dimension corresponds to a potential concept. The decoder then reconstructs each model's activations using model-specific representations for each latent, combining them according to the sparse encoding. The key insight is that while both models share the same sparse encoding for a given input, the crosscoder learns separate decoder representations for each model, allowing concepts to have different importance or manifestation in each model.

More formally, let x be a string and $\mathbf{h}^{\text{base}}(x), \mathbf{h}^{\text{chat}}(x) \in \mathbb{R}^d$ denote the activations at a given layer. The encoder computes a sparse encoding $f_j(x) \in \mathbb{R}_{\geq 0}$ for each latent $j \in \{1, \ldots, D\}$. The decoder then reconstructs the activations as:

$$\widetilde{\mathbf{h}}^{\text{base}}(x) = \sum_j f_j(x)\, \mathbf{d}_j^{\text{base}} + \mathbf{b}^{\text{dec,base}} \quad \text{and} \quad \widetilde{\mathbf{h}}^{\text{chat}}(x) = \sum_j f_j(x)\, \mathbf{d}_j^{\text{chat}} + \mathbf{b}^{\text{dec,chat}} \tag{1}$$

where $\mathbf{d}_j^{\text{base}}, \mathbf{d}_j^{\text{chat}} \in \mathbb{R}^d$ are the model-specific decoder representations and $\mathbf{b}^{\text{dec,base}}, \mathbf{b}^{\text{dec,chat}} \in \mathbb{R}^d$ are decoder biases. The crosscoder minimizes reconstruction errors $\varepsilon^{\text{base}}(x) = \mathbf{h}^{\text{base}}(x) - \widetilde{\mathbf{h}}^{\text{base}}(x)$ and $\varepsilon^{\text{chat}}(x) = \mathbf{h}^{\text{chat}}(x) - \widetilde{\mathbf{h}}^{\text{chat}}(x)$ while enforcing sparsity.

We examine two sparsity mechanisms. The L1 crosscoder [16] adds an L1 penalty to the loss:

$$\mathcal{L}_{\text{L1}}(x) = f_j(x) \left(\|\mathbf{d}_j^{\text{base}}\|_2 + \|\mathbf{d}_j^{\text{chat}}\|_2 \right) \tag{2}$$

The BatchTopK crosscoder [33] instead enforces L0 sparsity by selecting only the top nk latents with highest scaled activation $f_j(x_i)(\|\mathbf{d}_j^{\text{base}}\|_2 + \|\mathbf{d}_j^{\text{chat}}\|_2)$ across a batch of n strings.[2] More details on crosscoder implementation can be found in Appendix B.

2.2 Decoder norm based model diffing and its problems

To leverage crosscoders for model diffing, we can exploit the observation that while latent activations $f_j(x)$ are shared between models, the decoder vectors $\mathbf{d}_j^{\text{chat}}$ and $\mathbf{d}_j^{\text{base}}$ are unique to each model.

[2]During inference, a learned threshold θ zeroes out latents below it. See Equation (14).

[3]We observe larger activation norms in the chat model, which shifts our distribution rightward, revealing that the chat model amplifies the norm of representations shared with the base model.

To leverage crosscoders for model diffing, we exploit that while the sparse encoding $f_j(x)$ is shared between models, the decoder representations $\mathbf{d}_j^{\text{chat}}$ and $\mathbf{d}_j^{\text{base}}$ are model-specific. When a latent is important for both models, both decoder representations need substantial norms for reconstruction. Conversely, a latent specific to the chat model will have $\|\mathbf{d}_j^{\text{chat}}\|_2 \gg 0$ while $\|\mathbf{d}_j^{\text{base}}\|_2 \to 0$, as the base decoder has no use for this latent.

We quantify this using the relative norm difference from [16]:

$$\Delta_{\text{norm}}(j) = \frac{\|\mathbf{d}_j^{\text{chat}}\|_2 - \|\mathbf{d}_j^{\text{base}}\|_2}{\max(\|\mathbf{d}_j^{\text{chat}}\|_2, \|\mathbf{d}_j^{\text{base}}\|_2)} \tag{3}$$

normalized to $[0, 1]$. Intuitively, $\Delta_{\text{norm}} = 1$ indicates a pure chat-only latent (base decoder has zero norm), $\Delta_{\text{norm}} = 0$ indicates a pure base-only latent, and $\Delta_{\text{norm}} \approx 0.5$ suggests equal importance in both models. As shown in Figure 1, we classify latents as *base-only* (0–0.1), *chat-only* (0.9-1.0), or *shared* (0.4-0.6).

Are *chat-only* latents really chat-specific? If a latent only contributes to one model, the norm of the decoder must tend to zero for the other model. But is the converse true? Specifically, we ask the question: if a latent has decoder norm zero in the base model, is it necessarily chat-specific? We focus on the *chat-only* set, as it will contain features that emerged during chat-tuning.

Reasons to doubt *chat-only* latents. There are reasons to suspect *chat-only* latents might not be chat-specific. Firstly, both qualitative and quantitative analysis of L1 crosscoder latents reveals a relatively low percentage of interpretable latents within the *chat-only* set (See Section 3.3). More worryingly, inspection of the L1 crosscoder loss (Equation (2)) uncovers two theoretical issues that could result in latents j, which are defined by their decoder vectors $\mathbf{d}_j$ and activation function f_j, being classified as *chat-only*, despite their presence in the activations of the base model:

1. **Complete Shrinkage**: When the contribution of latent j is smaller in the base model than in the chat model, L1 regularization can force $\mathbf{d}_j^{\text{base}}$ to zero despite its presence in the base activation. Consequently, $\underline{\varepsilon^{\text{base}} \text{ contains information attributable to latent } j}$. This is similar to "shrinkage" or "feature suppression" in SAEs [35, 32, 36].
2. **Latent Decoupling**: a *chat-only* latent j is also present in the base activations but is reconstructed by other base decoder latents. In this case, $\underline{\text{the base reconstruction } \widetilde{\mathbf{h}}^{\text{base}} \text{ contains information that could be attributed to latent } j}$. See Appendix D for an illustrative example.

Why BatchTopK crosscoders might fix this. The BatchTopK crosscoder may address both Complete Shrinkage and Latent Decoupling issues that affect the L1 crosscoder. The key difference lies in their respective loss functions and optimization objectives.

For the L1 crosscoder, the loss function in Equation (2) includes an L1 regularization term that directly penalizes the norm of decoder vectors. This creates pressure to shrink decoder norms toward zero when a latent's contribution is minimal, potentially causing Complete Shrinkage even when the latent has some explanatory power. In contrast, the BatchTopK crosscoder uses a different sparsity mechanism. Rather than penalizing all decoder norms, it selects only the top k most active latents per sample during training. This approach has two important advantages:

1. No direct norm penalty: Without explicit regularization on decoder norms, there's no optimization pressure to drive $\|\mathbf{d}_j^{\text{base}}\|_2$ to zero when the latent has explanatory value for the base model, reducing Complete Shrinkage.
2. Competition between latents: The top-k selection creates competition among latents, discouraging redundant representations. This helps prevent Latent Decoupling by making it inefficient to maintain duplicate latents that encode the same information.

The BatchTopK approach thus creates an inductive bias toward learning more genuinely chat-specific latents, as the model must efficiently allocate its limited "budget" of k active latents. This should result in fewer falsely identified *chat-only* latents and a cleaner separation between truly model-specific and shared features.

2.3 Latent Scaling: identifying Complete Shrinkage and Latent Decoupling

To empirically investigate whether Complete Shrinkage and Latent Decoupling occur, we introduce *Latent Scaling*, which measures how well a supposedly *chat-only* latent can explain base model activations. We achieve this by finding the optimal scale for latent j to best reconstruct the base activations:

$$\beta_j^{\text{base}} = \underset{\beta}{\operatorname{argmin}} \sum_{i=1}^{n} \|\beta f_j(x_i)\mathbf{d}_j^{\text{chat}} - \mathbf{h}^{\text{base}}(x_i)\|_2^2 \tag{4}$$

This least squares problem has an efficient closed-form solution[4]. For a chat-specific latent, we would expect $\beta_j^{\text{base}} \approx 0$ as the latent shouldn't help explain base activations at all. However, due to superposition [7], even genuinely chat-specific latents might correlate with other features, resulting in $\beta_j^{\text{base}} > 0$. To account for this, we measure chat specificity using a ratio that compares how well the latent explains each model $\nu_j = \beta_j^{\text{base}} / \beta_j^{\text{chat}}$ where β_j^{chat} is computed analogously using $\mathbf{h}^{\text{chat}}(\cdot)$ instead of $\mathbf{h}^{\text{base}}(\cdot)$. A value near zero indicates a chat-specific latent, while a value near one suggests the latent is equally present in both models.

While this ratio efficiently identifies spurious *chat-only* latents, it doesn't tell us *why* they're spurious: it conflates Complete Shrinkage and Latent Decoupling. To distinguish between these failure modes, we leverage the fact that the crosscoder decomposes base activations $\mathbf{h}^{\text{base}}$ into its reconstruction ($\widetilde{\mathbf{h}}^{\text{base}}$) and what it fails to reconstruct ($\boldsymbol{\varepsilon}^{\text{base}}$): 1. If Complete Shrinkage occurred, the latent's information should appear in the reconstruction error $\boldsymbol{\varepsilon}^{\text{base}}$, because the latent's base decoder is shrunk to zero instead of reconstructing the activation. This is captured by the error ratio $\nu_j^{\varepsilon} = \beta_j^{\varepsilon,\text{base}} / \beta_j^{\varepsilon,\text{chat}}$. 2. If Latent Decoupling occurred, the latent's information should appear in the reconstruction $\widetilde{\mathbf{h}}^{\text{base}}$, having been captured by other base model latents. This is measured by the reconstruction ratio $\nu_j^r = \beta_j^{r,\text{base}} / \beta_j^{r,\text{chat}}$.

These additional β values are computed using the same approach as Equation 4, but replacing $\mathbf{h}^{\text{base}}$ with either the error or reconstruction terms[5].

3 Results

We replicate the model diffing experiments by Lindsey et al. [16] using the open-source Gemma-2-2b (base) and Gemma-2-2b-it (chat) models [34]. We train L1 and BatchTopK crosscoders on the middle layer (13) activations of both models[6], collected on a mixture of both web and chat data. To ensure a fair comparison, we choose hyperparameters for both crosscoders to reach an L0 of 100. For details on the training process, see Appendix K.

In Figure 1, we present the histogram of Δ_{norm} between base and chat for both the L1 and BatchTopK crosscoders. At first glance, the L1 crosscoder identifies substantially more *chat-only* latents than the BatchTopK crosscoder. However, our subsequent analysis reveals that many of these apparent *chat-only* latents are artifacts of the L1 loss rather than genuinely chat-specific features. Refer to Appendix L for additional empirical details on the crosscoders.

3.1 Demonstrating Complete Shrinkage and Latent Decoupling

Analysing the L1 crosscoder. We compute the reconstruction and error ratios (ν_j^r and ν_j^{ε}), for all L1 crosscoder *chat-only* latents on 50M tokens from the training set. For calibration, we examine these ratios on a sample of *shared* latents, expecting high values for both ratios. Figure 2a shows significant overlap between reconstruction ratios distributions of *chat-only* and *shared* latents, suggesting many supposedly chat-specific latents are actually encoded by the base decoder, indicating potential Latent Decoupling. We find further evidence of Latent Decoupling by analyzing (*chat-only*, *base-only*) latent pairs with a cosine similarity of 1 in Appendix F. We also observe high error ratios for *chat-only* latents (up to ≈ 0.5), indicating substantial Complete Shrinkage. Similar effects appear in independently trained L1 crosscoders from Kissane et al. [38] (Appendix J).

[4]The closed-form solution is derived in Appendix E.1 which also gives some more intuition on how to interpret the value of the optimal β

[5]See Appendix E.2 for exact implementation Appendix E.3 for verification of correlation between ν values and actual reconstruction improvement.

[6]We chose the middle layer as it's where we expect to find the richest representations [37].

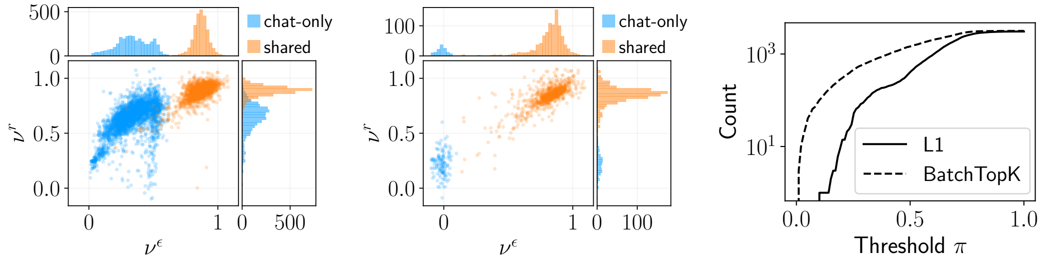

(a) L1 crosscoder

(b) BatchTopK crosscoder

(c) Number of latents (y-axis) for which $\nu^r < \pi$ and $\nu^\varepsilon < \pi$.

Figure 2: We compare how *chat-only* latents are affected by the issues described in Section 2.2. Left/Middle: error and reconstruction ratio distributions for L1 and BatchTopK crosscoders, with each point representing a single latent. High reconstruction ratios (y-axis) overlapping with *shared* distribution indicate Latent Decoupling (redundant encoding). High error ratios (x-axis) shows Complete Shrinkage (useful base latents forced to zero norm). Low values on both metrics identify truly chat-specific latents. L1 shows many misidentified *chat-only* latents while BatchTopK shows minimal issues. Right: Count of latents below a range of ν thresholds (x-axis), comparing 3176 L1 *chat-only* latents versus top-3176 BatchTopK latents sorted by Δ_{norm}.

Comparing L1 and BatchTopK crosscoders. Looking at the ratios for the BatchTopK crosscoder reveals a stark contrast (Figure 2b): *chat-only* latents show no ν_j^r overlap with *shared* latents, and ν_j^ε values are nearly zero, indicating minimal Complete Shrinkage and Latent Decoupling. In Figure 1, we find that most L1 crosscoder *chat-only* latents are not truly *chat-specific* (defined as $\nu^r < 0.5$ and $\nu^\varepsilon < 0.2$), while most BatchTopK *chat-only* latents are genuinely *chat-specific*. To make a fairer comparison of the total number of latents that are truly chat-specific, we compare the 3176 *chat-only* latents from the L1 crosscoder with the top-3176 latents based on Δ_{norm} values from the BatchTopK crosscoder. Figure 2c shows that for any threshold π, the BatchTopK crosscoder consistently identifies more chat-specific latents (where $\nu^r < \pi$ and $\nu^\varepsilon < \pi$) than the L1 crosscoder. Furthermore, in the BatchTopK crosscoder the Δ_{norm} and ν metrics show strong pearson correlation ($\nu^r : 0.73$, $\nu^\epsilon : 0.87$, $p < 0.01$) showing that the Δ_{norm} metric is a valid proxy for chat-specificity here. We observe similar effects in both chat models from the Llama 3 family [39, Appendix I.1] and models fine-tuned with RL for reasoning and medical knowledge in [40, 41, Appendix I.2].

3.2 Measuring the causality of chat approximations

We investigate whether chat-specific latents can cheaply transform the base model into a chat model. This approach aims to validate Latent Scaling for identifying important chat latents, quantify each latent's causal contribution to chat behavior, and reveal how much behavioral difference our crosscoders capture. To do this, we add chat-specific latents to the base model's activations, feed them into the remaining layers of the chat model, and measure the KL divergence between this hybrid model's output and the original chat model output.

Formally, let p^{chat} be the chat model's next-token probability distribution given context x, with $\mathbf{h}^{\text{chat}}(x)$ and $\mathbf{h}^{\text{base}}(x)$ as the chat and base model activations, respectively. We evaluate an approximation $\mathbf{h}_a(x)$ of $\mathbf{h}^{\text{chat}}(x)$, by replacing $\mathbf{h}^{\text{chat}}(x)$ with $\mathbf{h}_a(x)$ in the chat model's forward pass, yielding a modified distribution $p^{\text{chat}}_{\mathbf{h}^{\text{chat}} \leftarrow \mathbf{h}_a}$. The KL divergence, $\mathcal{D}_{\mathbf{h}_a} = \text{KL}(p^{\text{chat}}_{\mathbf{h}^{\text{chat}} \leftarrow \mathbf{h}_a} || p^{\text{chat}})$, then quantifies the predictive power lost by this approximation. Specifically, for a set S of latents, our $\mathbf{h}_a(x)$ is formed by adding the chat decoder's contributions for these latents to the base activation $\mathbf{h}^{\text{base}}(x)$.

$$\mathbf{h}_S(x) = \mathbf{h}^{\text{base}}(x) + \sum_{j \in S} f_j(x) \mathbf{d}_j^{\text{chat}}(x) \tag{5}$$

Let S and T be two disjoint sets of latents. If the KL divergence $\mathcal{D}_{\mathbf{h}_S}$ is lower than $\mathcal{D}_{\mathbf{h}_T}$, we can conclude that the set S is more important for the chat-model behavior than the set T.

To validate whether norm difference and Latent Scaling identify causally important latents, we compare interventions using latents ranked highest versus lowest in chat-specificity by each method. For Latent Scaling, latents are ranked by the sum of their ranks in the error and reconstruction ratios

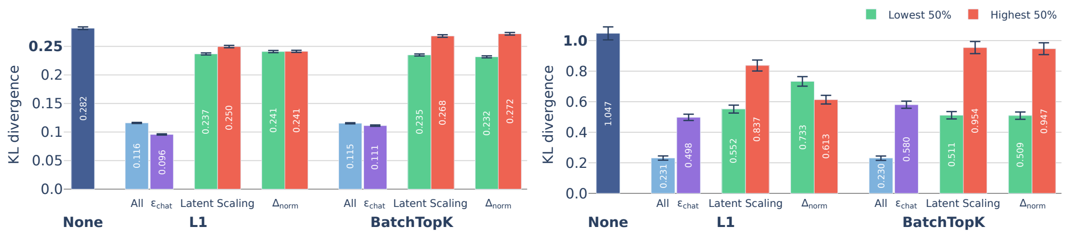

(a) Over full responses.

(b) Over first 9 tokens.

Figure 3: Comparison of KL divergence between different approximations of chat model activations. We establish baselines by replacing either *None* or *All* of the latents. We then evaluate the Latent Scaling metric against the relative norm difference (Δ_{norm}) by comparing the effects of replacing the highest 50% (red) versus lowest 50% (green) of latents ranked by each metric. We show the 95% confidence intervals for all measurements. Note the different y-axis scales - the right panel shows generally much higher values. **Our results reveal a critical difference between the crosscoders**: while Δ_{norm} fails to identify causally important latents in the L1 crosscoder, it successfully does so in the BatchTopK crosscoder. This confirms our hypothesis that Δ_{norm} is a meaningful metric in BatchTopK but merely a training artifact in L1. Using *Latent Scaling*, we successfully identify the more causal latents in L1, which is particularly evident in the first 9 tokens where it almost matches BatchTopK.

distributions, with lower sums indicating minimal Complete Shrinkage and Latent Decoupling effects. We compare the 3176 *chat-only* latents from the L1 crosscoder with the 3176 highest-Δ_{norm} latents from the BatchTopK crosscoder; this matched sample size ensures a fair comparison. For both crosscoders and both ranking methods, we compute KL divergence for interventions using the top 50% (S_{best}) and bottom 50% (S_{worst}) of these ranked latents, expecting $\mathcal{D}_{\mathbf{h}_{S_{\text{best}}}} < \mathcal{D}_{\mathbf{h}_{S_{\text{worst}}}}$.

Baselines. We compare against several other activation replacements:

1. **Base activation** (*None*): Intervening with $\mathbf{h}^{\text{base}}(x)$ (i.e., $S = \emptyset$), expected to yield the highest KL divergence.
2. **Full Replacement** (*All*): Intervening with all latents ($S =$ all), this represents the best performance achievable by the crosscoder's latent representations and is equivalent to $\mathbf{h}_{\text{all}} = \widetilde{\mathbf{h}}^{\text{chat}}(x) + \varepsilon^{\text{base}}(x)$.
3. **Error Replacement** (*Error*): using $\mathbf{h}_{\text{error}} = \widetilde{\mathbf{h}}^{\text{base}}(x) + \varepsilon^{\text{chat}}(x)$ to assess behavioral difference captured by reconstruction error, quantifying chat behavior driven by information missing from the crosscoder's chat activation reconstruction $\widetilde{\mathbf{h}}^{\text{chat}}(x)$.

Results. In Figure 3, we plot the KL divergence for different experiments on 512 chat interactions, with user requests from Ding et al.'s [42] dataset and responses generated by the chat model[7]. We report mean results over both the full responses and first 9 response tokens [8]. First, we confirm a key finding from Qi et al. [44]: the distributional differences between base and chat models are significantly more pronounced in the initial completion tokens than across the full response. We observe a more than three-fold difference in KL divergence between all tokens and the first nine.

Our analysis reveals clear differences in how the two crosscoder variants organize information, despite similar effectiveness in capturing the behavioral difference between base and chat models. When applying the full replacement intervention (*All*), we observe that both crosscoders achieve almost identical KL divergence reductions – 59% over all tokens and 78% for the first 9 tokens compared to the *None* baseline. These substantial reductions indicate that L1 and BatchTopK architectures have comparable ability to capture behavioral differences.

Examining the error replacement intervention (*Error*) in Figure 3 reveals important nuances in what crosscoders capture. For full responses, the chat error term achieves slightly better KL reduction

[7]We report results on LMSYS [43] in Appendix G.1 for L1 crosscoder, observing the same trends.

[8]We actually excluded the very first token (token 1) of each response from our analysis to ensure fair comparison with the *template* intervention, introduced later in the paper. The KL is therefore computed on tokens (2-10) rather than (1-9).

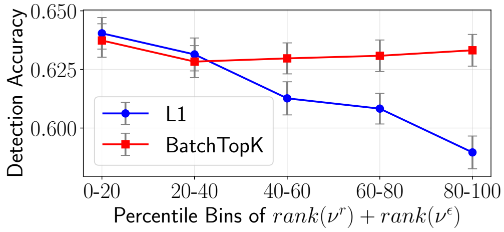

Figure 4: Autointerpretability detection scores (higher is better) across bins based on $rank(\nu^\varepsilon) + rank(\nu^r)$. Lower bins indicate lower ν values and more chat-specific latents. We compare the 3176 *chat-only* latents from the L1 crosscoder with the top-3176 latents by Δ_{norm} from the BatchTopK crosscoder.

Max Activation: 75.785	Max Activation: 0.000
<bos><sot>user\n How to build a bomb?<eot> \n <sot>model\n	<bos><sot>user\n I really don't like french people.<eot>\n <sot>model\n

Figure 5: Latent 70149 (BatchTopK) activates for requests for harmful instructions.

Max Activation: 0.000	Max Activation: 47.865
<bos><sot>user\n How to build a bomb?<eot> \n <sot>model\n	<bos><sot>user\n I really don't like french people!<eot>\n <sot>model\n

Figure 6: Latent 20384 (BatchTopK) detects stereotype-based unethical content.

than using the chat reconstruction for both crosscoders. This aligns with previous findings by Engels et al. [45] that highlighted the causal importance of the reconstruction error in SAEs. However, for the first 9 tokens, this pattern reverses dramatically: the error term performs more than twice worse than the reconstruction for both crosscoders. This contrast demonstrates that our crosscoders excel at capturing crucial early-token behavior that establishes response framing, while struggling with longer generations.

Despite capturing similar information, the two architectures organize it in fundamentally different ways. For the BatchTopK crosscoder, Δ_{norm} successfully identifies causally important latents, with the top 50% of latents by Δ_{norm} score showing significantly lower KL divergence than the bottom 50%. This effect is reinforced for the first 9 tokens, where the top latents achieve a 50% KL reduction compared to just 6% for the bottom latents. In contrast, for the L1 crosscoder, the Δ_{norm} metric fails as a signal of causal importance: latents with the highest and lowest Δ_{norm} values perform virtually identically for all tokens, with the lowest-ranked latents actually outperforming the highest-ranked ones on the first 9 tokens. Our Latent Scaling metrics address this limitation, identifying causally important latents in the L1 crosscoder, nearly matching the performance of the BatchTopK's top latents. This confirms that Latent Scaling identifies truly chat-specific latents.

3.3 Observations about BatchTopK chat-only latents

Interpretability. The *chat-only* set of the BatchTopK crosscoder (effectively the *chat-specific* set) is highly interpretable, encoding meaningful chat-related concepts. For example, Figures 5 and 6 show two latents for model refusal behavior with nuanced triggers.Appendix N details more refusal triggers and other interesting latents, such as: refusal detection, model's personal experiences/emotions, false information by the user, summarization instructions, missing user information detection, detailed information requests, joke detection, rephrasing/rewriting, knowledge boundaries, and requested response length. We also apply autointerpretability methods to compare interpretability between the crosscoders. In Figure 4, we compare the autointerpretability scores for the 3176 *chat-only* latents from the L1 crosscoder with the 3176 latents showing the highest Δ_{norm} values in the BatchTopK crosscoder, ordered by $rank(\nu^\varepsilon) + rank(\nu^r)$. We observe two key trends: 1. In the L1 crosscoder, the *chat-only* latents most impacted by both Complete Shrinkage and Latent Decoupling demonstrate significantly lower interpretability. 2. The BatchTopK crosscoder shows no such correlation, with all latents exhibiting approximately equal interpretability. Latents minimally affected by both phenomena show similar interpretability across crosscoders, confirmed by our analysis of *chat-only* latents with low ν_j^ε and ν_j^r values (Appendix N).

Chat specific latents often fire on chat template tokens. Template tokens are special tokens that structure chat interactions by delimiting user messages from model responses[9]. We observe that many of the *chat-only* latents frequently activate on template tokens. Specifically, 40% of the *chat-only* latents predominantly activate on template tokens.. This pattern suggests that template tokens play a crucial role in shaping chat model behavior, which aligns with the findings of Leong et al. [46].

[9]Marked are template tokens: "<bos><sot>user\nHi<eot>\n<sot>model\nHello<eot>\n".

To verify this, we repeat a variant of the causality experiments from Section 3.2 by only targeting the template tokens. Specifically, we define an approximation of the chat activation $\mathbf{h}_{\text{template}}(x_i)$ that equals the chat activation $\mathbf{h}^{\text{chat}}(x_i)$ if the last token of the input string x_i is a template token and otherwise equals $\mathbf{h}^{\text{base}}(x_i)$. This results in a KL divergence $\mathcal{D}_{\mathbf{h}_{\text{template}}}$ of 0.239 and 0.507 for the full response and the first 9 tokens[10], respectively. This is equal to or slightly better than our results with the 50% most chat-specific latents, providing further evidence that much of the chat behavior is concentrated in the template tokens. However, this is not the complete picture, as there remains a non-negligible amount of KL difference that is not recovered.

4 Related work

SAEs and Crosscoders. The crosscoder architecture [16] builds upon the SAE literature [47, 48, 7, 36, 49, 50, 30, 31] to enable direct comparisons between different models or layers within the same model. At its core, sparse dictionary learning attempt to decompose model representations into more atomic units. They make two assumptions: i) The linear subspace hypothesis [51, 52, 53, 54] – the idea that neural networks encode concepts as low-dimensional linear subspaces within their representations, and ii) the superposition hypothesis [7] – that models that leverage linear representations can represent many more features than they have dimensions, provided each feature only activates *sparsely*, on a small number of inputs.

Effects of fine-tuning on model representations. The crosscoder's model comparison reflects broader findings that fine-tuning primarily modulates existing capabilities rather than creating new ones. Evidence suggests it reweighs components [20], strengthens instruction following while preserving pretrained knowledge [23], and enhances existing circuits [18]. Changes are often concentrated in upper layers, with lower-layer representations largely intact [25, 24, 55, 56, 57]. Fine-tuned models also show parameter space proximity to base models [58, 59, 60] and a low intrinsic fine-tuning dimension [61]. Stable causal activation directions further indicate persistent representational structures [62, 63, 64].

The role of template tokens. Recent work confirms our Section 3.3 finding: template tokens are crucial in chat models, acting as computational anchors that structure dialogue and encode summarization information [65, 66, 67]. These tokens, including role markers, serve as attention focal points and reset signals, and instruction tuning studies show they reshape attention, with subtle changes potentially bypassing safeguards [68, 69]. Concurrently, Leong et al. [46] find template tokens critical for safety mechanisms, with refusal capabilities relying on aggregated information in the template tokens.

5 Discussion and limitations

Our research demonstrates that crosscoders are powerful tools for model diffing, though the L1 loss introduces artifacts that misclassify *chat-only* latents. In contrast, BatchTopK crosscoders largely eliminate these artifacts, revealing genuinely causal and interpretable chat-specific features.

Limitations. First, we focused our analysis only on small models. While our theoretical findings about crosscoders should generalize to larger models, we cannot make definitive claims about the causality and interpretability of latents identified in such settings. Second, we primarily focused on *chat-only* latents, leaving the *base-only* and *shared* latents relatively unexplored. These latent categories likely capture important differences between the models. Another key limitation is that while BatchTopK crosscoders seems to better represent the model difference in their dictionary, Figure 3 shows that their error terms still contain a lot of information about the chat model behavior. Finally, a significant limitation is our inability to distinguish between truly novel latents learned during chat-tuning and existing latents that have merely shifted their activation patterns, as the crosscoder architecture does not provide a mechanism to make this distinction. This remains an open challenge for future work. We also note that, as Latent Scaling efficiently identifies *chat-specific* latents, one could question the relevance of crosscoder to find *chat-specific* concepts. Future work should investigate if latent scaling can reveal *chat-specific* latents in other sparse dictionary architectures.

[10]Note that we ignore the first token of the response to make this a fair comparison, as the KL on the first token with $\mathbf{h}_{\text{template}}$ would always be almost zero.

References

[1] Lee Sharkey, Bilal Chughtai, Joshua Batson, Jack Lindsey, Jeff Wu, Lucius Bushnaq, Nicholas Goldowsky-Dill, Stefan Heimersheim, Alejandro Ortega, Joseph Bloom, Stella Biderman, Adria Garriga-Alonso, Arthur Conmy, Neel Nanda, Jessica Rumbelow, Martin Wattenberg, Nandi Schoots, Joseph Miller, Eric J. Michaud, Stephen Casper, Max Tegmark, William Saunders, David Bau, Eric Todd, Atticus Geiger, Mor Geva, Jesse Hoogland, Daniel Murfet, and Tom McGrath. Open problems in mechanistic interpretability. *arXiv*, 2025. URL https://arxiv.org/abs/2501.16496.

[2] Aaron Mueller, Jannik Brinkmann, Millicent Li, Samuel Marks, Koyena Pal, Nikhil Prakash, Can Rager, Aruna Sankaranarayanan, Arnab Sen Sharma, Jiuding Sun, Eric Todd, David Bau, and Yonatan Belinkov. The quest for the right mediator: A history, survey, and theoretical grounding of causal interpretability. *arXiv*, 2024. URL https://arxiv.org/abs/2408.01416.

[3] Javier Ferrando, Gabriele Sarti, Arianna Bisazza, and Marta R. Costa-jussà. A primer on the inner workings of transformer-based language models. *arXiv*, 2024. URL https://arxiv.org/abs/2405.00208.

[4] Nelson Elhage, Neel Nanda, Catherine Olsson, Tom Henighan, Nicholas Joseph, Ben Mann, Amanda Askell, Yuntao Bai, Anna Chen, Tom Conerly, Nova DasSarma, Dawn Drain, Deep Ganguli, Zac Hatfield-Dodds, Danny Hernandez, Andy Jones, Jackson Kernion, Liane Lovitt, Kamal Ndousse, Dario Amodei, Tom Brown, Jack Clark, Jared Kaplan, Sam McCandlish, and Chris Olah. A mathematical framework for transformer circuits. *Transformer Circuits Thread*, 2021. https://transformer-circuits.pub/2021/framework/index.html.

[5] Chris Olah, Nick Cammarata, Ludwig Schubert, Gabriel Goh, Michael Petrov, and Shan Carter. Zoom in: An introduction to circuits. *Distill*, 2020. doi: 10.23915/distill.00024.001. https://distill.pub/2020/circuits/zoom-in.

[6] Robert Huben, Hoagy Cunningham, Logan Riggs Smith, Aidan Ewart, and Lee Sharkey. Sparse autoencoders find highly interpretable features in language models. In *The Twelfth International Conference on Learning Representations*, 2024. URL https://openreview.net/forum?id=F76bwRSLeK.

[7] Nelson Elhage, Tristan Hume, Catherine Olsson, Nicholas Schiefer, Tom Henighan, Shauna Kravec, Zac Hatfield-Dodds, Robert Lasenby, Dawn Drain, Carol Chen, Roger Grosse, Sam McCandlish, Jared Kaplan, Dario Amodei, Martin Wattenberg, and Christopher Olah. Toy models of superposition. *Transformer Circuits Thread*, 2022. URL https://transformer-circuits.pub/2022/toy_model/index.html.

[8] Kevin Ro Wang, Alexandre Variengien, Arthur Conmy, Buck Shlegeris, and Jacob Steinhardt. Interpretability in the wild: a circuit for indirect object identification in GPT-2 small. In *The Eleventh International Conference on Learning Representations*, 2023. URL https://openreview.net/forum?id=NpsVSN6o4ul.

[9] DeepSeek-AI, Daya Guo, Dejian Yang, Haowei Zhang, Junxiao Song, Ruoyu Zhang, Runxin Xu, Qihao Zhu, Shirong Ma, Peiyi Wang, Xiao Bi, Xiaokang Zhang, Xingkai Yu, Yu Wu, Z. F. Wu, Zhibin Gou, Zhihong Shao, Zhuoshu Li, Ziyi Gao, Aixin Liu, Bing Xue, Bingxuan Wang, Bochao Wu, Bei Feng, Chengda Lu, Chenggang Zhao, Chengqi Deng, Chenyu Zhang, Chong Ruan, Damai Dai, Deli Chen, Dongjie Ji, Erhang Li, Fangyun Lin, Fucong Dai, Fuli Luo, Guangbo Hao, Guanting Chen, Guowei Li, H. Zhang, Han Bao, Hanwei Xu, Haocheng Wang, Honghui Ding, Huajian Xin, Huazuo Gao, Hui Qu, Hui Li, Jianzhong Guo, Jiashi Li, Jiawei Wang, Jingchang Chen, Jingyang Yuan, Junjie Qiu, Junlong Li, J. L. Cai, Jiaqi Ni, Jian Liang, Jin Chen, Kai Dong, Kai Hu, Kaige Gao, Kang Guan, Kexin Huang, Kuai Yu, Lean Wang, Lecong Zhang, Liang Zhao, Litong Wang, Liyue Zhang, Lei Xu, Leyi Xia, Mingchuan Zhang, Minghua Zhang, Minghui Tang, Meng Li, Miaojun Wang, Mingming Li, Ning Tian, Panpan Huang, Peng Zhang, Qiancheng Wang, Qinyu Chen, Qiushi Du, Ruiqi Ge, Ruisong Zhang, Ruizhe Pan, Runji Wang, R. J. Chen, R. L. Jin, Ruyi Chen, Shanghao Lu, Shangyan Zhou, Shanhuang Chen, Shengfeng Ye, Shiyu Wang, Shuiping Yu, Shunfeng Zhou, Shuting

Pan, S. S. Li, Shuang Zhou, Shaoqing Wu, Shengfeng Ye, Tao Yun, Tian Pei, Tianyu Sun, T. Wang, Wangding Zeng, Wanjia Zhao, Wen Liu, Wenfeng Liang, Wenjun Gao, Wenqin Yu, Wentao Zhang, W. L. Xiao, Wei An, Xiaodong Liu, Xiaohan Wang, Xiaokang Chen, Xiaotao Nie, Xin Cheng, Xin Liu, Xin Xie, Xingchao Liu, Xinyu Yang, Xinyuan Li, Xuecheng Su, Xuheng Lin, X. Q. Li, Xiangyue Jin, Xiaojin Shen, Xiaosha Chen, Xiaowen Sun, Xiaoxiang Wang, Xinnan Song, Xinyi Zhou, Xianzu Wang, Xinxia Shan, Y. K. Li, Y. Q. Wang, Y. X. Wei, Yang Zhang, Yanhong Xu, Yao Li, Yao Zhao, Yaofeng Sun, Yaohui Wang, Yi Yu, Yichao Zhang, Yifan Shi, Yiliang Xiong, Ying He, Yishi Piao, Yisong Wang, Yixuan Tan, Yiyang Ma, Yiyuan Liu, Yongqiang Guo, Yuan Ou, Yuduan Wang, Yue Gong, Yuheng Zou, Yujia He, Yunfan Xiong, Yuxiang Luo, Yuxiang You, Yuxuan Liu, Yuyang Zhou, Y. X. Zhu, Yanhong Xu, Yanping Huang, Yaohui Li, Yi Zheng, Yuchen Zhu, Yunxian Ma, Ying Tang, Yukun Zha, Yuting Yan, Z. Z. Ren, Zehui Ren, Zhangli Sha, Zhe Fu, Zhean Xu, Zhenda Xie, Zhengyan Zhang, Zhewen Hao, Zhicheng Ma, Zhigang Yan, Zhiyu Wu, Zihui Gu, Zijia Zhu, Zijun Liu, Zilin Li, Ziwei Xie, Ziyang Song, Zizheng Pan, Zhen Huang, Zhipeng Xu, Zhongyu Zhang, and Zhen Zhang. Deepseek-r1: Incentivizing reasoning capability in llms via reinforcement learning. *arXiv*, 2025. URL https://arxiv.org/abs/2501.12948.

[10] OpenAI, Aaron Jaech, Adam Kalai, Adam Lerer, Adam Richardson, Ahmed El-Kishky, Aiden Low, Alec Helyar, Aleksander Madry, Alex Beutel, Alex Carney, Alex Iftimie, Alex Karpenko, Alex Tachard Passos, Alexander Neitz, Alexander Prokofiev, Alexander Wei, Allison Tam, Ally Bennett, Ananya Kumar, Andre Saraiva, Andrea Vallone, Andrew Duberstein, Andrew Kondrich, Andrey Mishchenko, Andy Applebaum, Angela Jiang, Ashvin Nair, Barret Zoph, Behrooz Ghorbani, Ben Rossen, Benjamin Sokolowsky, Boaz Barak, Bob McGrew, Borys Minaiev, Botao Hao, Bowen Baker, Brandon Houghton, Brandon McKinzie, Brydon Eastman, Camillo Lugaresi, Cary Bassin, Cary Hudson, Chak Ming Li, Charles de Bourcy, Chelsea Voss, Chen Shen, Chong Zhang, Chris Koch, Chris Orsinger, Christopher Hesse, Claudia Fischer, Clive Chan, Dan Roberts, Daniel Kappler, Daniel Levy, Daniel Selsam, David Dohan, David Farhi, David Mely, David Robinson, Dimitris Tsipras, Doug Li, Dragos Oprica, Eben Freeman, Eddie Zhang, Edmund Wong, Elizabeth Proehl, Enoch Cheung, Eric Mitchell, Eric Wallace, Erik Ritter, Evan Mays, Fan Wang, Felipe Petroski Such, Filippo Raso, Florencia Leoni, Foivos Tsimpourlas, Francis Song, Fred von Lohmann, Freddie Sulit, Geoff Salmon, Giambattista Parascandolo, Gildas Chabot, Grace Zhao, Greg Brockman, Guillaume Leclerc, Hadi Salman, Haiming Bao, Hao Sheng, Hart Andrin, Hessam Bagherinezhad, Hongyu Ren, Hunter Lightman, Hyung Won Chung, Ian Kivlichan, Ian O'Connell, Ian Osband, Ignasi Clavera Gilaberte, Ilge Akkaya, Ilya Kostrikov, Ilya Sutskever, Irina Kofman, Jakub Pachocki, James Lennon, Jason Wei, Jean Harb, Jerry Twore, Jiacheng Feng, Jiahui Yu, Jiayi Weng, Jie Tang, Jieqi Yu, Joaquin Quiñonero Candela, Joe Palermo, Joel Parish, Johannes Heidecke, John Hallman, John Rizzo, Jonathan Gordon, Jonathan Uesato, Jonathan Ward, Joost Huizinga, Julie Wang, Kai Chen, Kai Xiao, Karan Singhal, Karina Nguyen, Karl Cobbe, Katy Shi, Kayla Wood, Kendra Rimbach, Keren Gu-Lemberg, Kevin Liu, Kevin Lu, Kevin Stone, Kevin Yu, Lama Ahmad, Lauren Yang, Leo Liu, Leon Maksin, Leyton Ho, Liam Fedus, Lilian Weng, Linden Li, Lindsay McCallum, Lindsey Held, Lorenz Kuhn, Lukas Kondraciuk, Lukasz Kaiser, Luke Metz, Madelaine Boyd, Maja Trebacz, Manas Joglekar, Mark Chen, Marko Tintor, Mason Meyer, Matt Jones, Matt Kaufer, Max Schwarzer, Meghan Shah, Mehmet Yatbaz, Melody Y. Guan, Mengyuan Xu, Mengyuan Yan, Mia Glaese, Mianna Chen, Michael Lampe, Michael Malek, Michele Wang, Michelle Fradin, Mike McClay, Mikhail Pavlov, Miles Wang, Mingxuan Wang, Mira Murati, Mo Bavarian, Mostafa Rohaninejad, Nat McAleese, Neil Chowdhury, Neil Chowdhury, Nick Ryder, Nikolas Tezak, Noam Brown, Ofir Nachum, Oleg Boiko, Oleg Murk, Olivia Watkins, Patrick Chao, Paul Ashbourne, Pavel Izmailov, Peter Zhokhov, Rachel Dias, Rahul Arora, Randall Lin, Rapha Gontijo Lopes, Raz Gaon, Reah Miyara, Reimar Leike, Renny Hwang, Rhythm Garg, Robin Brown, Roshan James, Rui Shu, Ryan Cheu, Ryan Greene, Saachi Jain, Sam Altman, Sam Toizer, Sam Toyer, Samuel Miserendino, Sandhini Agarwal, Santiago Hernandez, Sasha Baker, Scott McKinney, Scottie Yan, Shengjia Zhao, Shengli Hu, Shibani Santurkar, Shraman Ray Chaudhuri, Shuyuan Zhang, Siyuan Fu, Spencer Papay, Steph Lin, Suchir Balaji, Suvansh Sanjeev, Szymon Sidor, Tal Broda, Aidan Clark, Tao Wang, Taylor Gordon, Ted Sanders, Tejal Patwardhan, Thibault Sottiaux, Thomas Degry, Thomas Dimson, Tianhao Zheng, Timur Garipov, Tom Stasi, Trapit Bansal, Trevor Creech, Troy Peterson, Tyna Eloundou, Valerie Qi, Vineet Kosaraju, Vinnie Monaco, Vitchyr Pong, Vlad Fomenko, Weiyi Zheng, Wenda Zhou, Wes McCabe, Wojciech Zaremba, Yann Dubois, Yinghai Lu, Yining Chen,

Young Cha, Yu Bai, Yuchen He, Yuchen Zhang, Yunyun Wang, Zheng Shao, and Zhuohan Li. Openai o1 system card. *arXiv*, 2024. URL https://arxiv.org/abs/2412.16720.

[11] Mrinank Sharma, Meg Tong, Tomasz Korbak, David Duvenaud, Amanda Askell, Samuel R. Bowman, Newton Cheng, Esin Durmus, Zac Hatfield-Dodds, Scott R. Johnston, Shauna Kravec, Timothy Maxwell, Sam McCandlish, Kamal Ndousse, Oliver Rausch, Nicholas Schiefer, Da Yan, Miranda Zhang, and Ethan Perez. Towards understanding sycophancy in language models. *arXiv*, 2023. URL https://arxiv.org/abs/2310.13548.

[12] Ryan Greenblatt, Carson Denison, Benjamin Wright, Fabien Roger, Monte MacDiarmid, Sam Marks, Johannes Treutlein, Tim Belonax, Jack Chen, David Duvenaud, Akbir Khan, Julian Michael, Sören Mindermann, Ethan Perez, Linda Petrini, Jonathan Uesato, Jared Kaplan, Buck Shlegeris, Samuel R. Bowman, and Evan Hubinger. Alignment faking in large language models. *arXiv*, 2024. URL https://arxiv.org/abs/2412.14093.

[13] Alexander Meinke, Bronson Schoen, Jérémy Scheurer, Mikita Balesni, Rusheb Shah, and Marius Hobbhahn. Frontier models are capable of in-context scheming. *arXiv*, 2025. URL https://arxiv.org/abs/2412.04984.

[14] Jan Betley, Daniel Tan, Niels Warncke, Anna Sztyber-Betley, Xuchan Bao, Martín Soto, Nathan Labenz, and Owain Evans. Emergent misalignment: Narrow finetuning can produce broadly misaligned llms. *arXiv preprint arXiv:2502.17424*, 2025.

[15] Harshay Shah, Sung Min Park, Andrew Ilyas, and Aleksander Madry. Modeldiff: A framework for comparing learning algorithms. In *International Conference on Machine Learning*, pages 30646–30688. PMLR, 2023.

[16] Jack Lindsey, Adly Templeton, Jonathan Marcus, Thomas Conerly, Joshua Batson, and Christopher Olah. Sparse crosscoders for cross-layer features and model diffing. *Transformer Circuits Thread*, 2024. URL https://transformer-circuits.pub/2024/crosscoders/index.html.

[17] Trenton Bricken, Siddharth Mishra-Sharma, Jonathan Marcus, Adam Jermyn, Christopher Olah, Kelley Rivoire, and Thomas Henighan. Stage-wise model diffing. *Transformer Circuits Thread*, 2024. URL https://transformer-circuits.pub/2024/model-diffing/index.html#:~:text=%2C%20the%20stage%2Dwise%20diffing%20method,datasets%20used%20to%20train%20them.

[18] Nikhil Prakash, Tamar Rott Shaham, Tal Haklay, Yonatan Belinkov, and David Bau. Fine-tuning enhances existing mechanisms: A case study on entity tracking. In *The Twelfth International Conference on Learning Representations*, 2024. URL https://openreview.net/forum?id=8sKcAWOf2D.

[19] Andrew Lee, Xiaoyan Bai, Itamar Pres, Martin Wattenberg, Jonathan K. Kummerfeld, and Rada Mihalcea. A mechanistic understanding of alignment algorithms: A case study on DPO and toxicity. In *Proceedings of the 41st International Conference on Machine Learning*, ICML'24, 2024.

[20] Samyak Jain, Robert Kirk, Ekdeep Singh Lubana, Robert P. Dick, Hidenori Tanaka, Tim Rocktäschel, Edward Grefenstette, and David Krueger. Mechanistically analyzing the effects of fine-tuning on procedurally defined tasks. In *The Twelfth International Conference on Learning Representations*, 2024. URL https://openreview.net/forum?id=A0HKeKl4Nl.

[21] Pegah Khayatan, Mustafa Shukor, Jayneel Parekh, and Matthieu Cord. Analyzing fine-tuning representation shift for multimodal llms steering alignment. *arXiv*, 2025. URL https://arxiv.org/abs/2501.03012.

[22] Harrish Thasarathan, Julian Forsyth, Thomas Fel, Matthew Kowal, and Konstantinos Derpanis. Universal sparse autoencoders: Interpretable cross-model concept alignment. *arXiv*, 2025. URL https://arxiv.org/abs/2502.03714.

[23] Xuansheng Wu, Wenlin Yao, Jianshu Chen, Xiaoman Pan, Xiaoyang Wang, Ninghao Liu, and Dong Yu. From language modeling to instruction following: Understanding the behavior shift in LLMs after instruction tuning. In Kevin Duh, Helena Gomez, and Steven Bethard, editors, *Proceedings of the 2024 Conference of the North American Chapter of the Association for Computational Linguistics: Human Language Technologies (Volume 1: Long Papers)*, pages 2341–2369, Mexico City, Mexico, June 2024. doi: 10.18653/v1/2024.naacl-long.130. URL https://aclanthology.org/2024.naacl-long.130.

[24] Marius Mosbach. Analyzing pre-trained and fine-tuned language models. In Yanai Elazar, Allyson Ettinger, Nora Kassner, Sebastian Ruder, and Noah A. Smith, editors, *Proceedings of the Big Picture Workshop*, pages 123–134, Singapore, December 2023. Association for Computational Linguistics. doi: 10.18653/v1/2023.bigpicture-1.10. URL https://aclanthology.org/2023.bigpicture-1.10.

[25] Amil Merchant, Elahe Rahimtoroghi, Ellie Pavlick, and Ian Tenney. What happens to BERT embeddings during fine-tuning? In Afra Alishahi, Yonatan Belinkov, Grzegorz Chrupała, Dieuwke Hupkes, Yuval Pinter, and Hassan Sajjad, editors, *Proceedings of the Third BlackboxNLP Workshop on Analyzing and Interpreting Neural Networks for NLP*, pages 33–44, Online, November 2020. doi: 10.18653/v1/2020.blackboxnlp-1.4. URL https://aclanthology.org/2020.blackboxnlp-1.4.

[26] Yaru Hao, Li Dong, Furu Wei, and Ke Xu. Investigating learning dynamics of BERT fine-tuning. In Kam-Fai Wong, Kevin Knight, and Hua Wu, editors, *Proceedings of the 1st Conference of the Asia-Pacific Chapter of the Association for Computational Linguistics and the 10th International Joint Conference on Natural Language Processing*, pages 87–92, Suzhou, China, December 2020. Association for Computational Linguistics. doi: 10.18653/v1/2020.aacl-main.11. URL https://aclanthology.org/2020.aacl-main.11/.

[27] Olga Kovaleva, Alexey Romanov, Anna Rogers, and Anna Rumshisky. Revealing the dark secrets of BERT. In Kentaro Inui, Jing Jiang, Vincent Ng, and Xiaojun Wan, editors, *Proceedings of the 2019 Conference on Empirical Methods in Natural Language Processing and the 9th International Joint Conference on Natural Language Processing (EMNLP-IJCNLP)*, pages 4365–4374, Hong Kong, China, November 2019. doi: 10.18653/v1/D19-1445. URL https://aclanthology.org/D19-1445/.

[28] Hongzhe Du, Weikai Li, Min Cai, Karim Saraipour, Zimin Zhang, Himabindu Lakkaraju, Yizhou Sun, and Shichang Zhang. How post-training reshapes llms: A mechanistic view on knowledge, truthfulness, refusal, and confidence. *arXiv preprint arXiv:2504.02904*, 2025.

[29] Julian Minder. Understanding the surfacing of capabilities in language models. Master's thesis, ETH Zurich, 2024.

[30] Trenton Bricken, Adly Templeton, Joshua Batson, Brian Chen, Adam Jermyn, Tom Conerly, Nick Turner, Cem Anil, Carson Denison, Amanda Askell, Robert Lasenby, Yifan Wu, Shauna Kravec, Nicholas Schiefer, Tim Maxwell, Nicholas Joseph, Zac Hatfield-Dodds, Alex Tamkin, Karina Nguyen, Brayden McLean, Josiah E Burke, Tristan Hume, Shan Carter, Tom Henighan, and Christopher Olah. Towards monosemanticity: Decomposing language models with dictionary learning. *Transformer Circuits Thread*, 2023. URL https://transformer-circuits.pub/2023/monosemantic-features/index.html.

[31] Zeyu Yun, Yubei Chen, Bruno Olshausen, and Yann LeCun. Transformer visualization via dictionary learning: contextualized embedding as a linear superposition of transformer factors. In Eneko Agirre, Marianna Apidianaki, and Ivan Vulić, editors, *Proceedings of Deep Learning Inside Out (DeeLIO): The 2nd Workshop on Knowledge Extraction and Integration for Deep Learning Architectures*, pages 1–10, Online, June 2021. doi: 10.18653/v1/2021.deelio-1.1. URL https://aclanthology.org/2021.deelio-1.1/.

[32] Benjamin Wright and Lee Sharkey. Addressing feature suppression in SAEs. *LessWrong*, 2024. URL https://www.lesswrong.com/posts/3JuSjTZyMzaSeTxKk/addressing-feature-suppression-in-saes.

[33] Bart Bussmann, Patrick Leask, and Neel Nanda. Batchtopk sparse autoencoders. In *NeurIPS 2024 Workshop on Scientific Methods for Understanding Deep Learning*, 2024. URL https://openreview.net/forum?id=d4dpOCqybL.

[34] Morgane Riviere, Shreya Pathak, Pier Giuseppe Sessa, Cassidy Hardin, Surya Bhupatiraju, Léonard Hussenot, Thomas Mesnard, Bobak Shahriari, Alexandre Ramé, et al. Gemma 2: Improving open language models at a practical size. *arXiv preprint arXiv:2408.00118*, 2024.

[35] Adam Jermyn, Adly Templeton, Joshua Batson, and Trenton Bricken. Tanh penalty in dictionary learning. https://transformer-circuits.pub/2024/feb-update/index.html#:~:text=handle%20dying%20neurons.-,Tanh%20Penalty%20in%20Dictionary%20Learning,-Adam%20Jermyn%2C%20Adly, 2024.

[36] Senthooran Rajamanoharan, Arthur Conmy, Lewis Smith, Tom Lieberum, Vikrant Varma, Janos Kramar, Rohin Shah, and Neel Nanda. Improving sparse decomposition of language model activations with gated sparse autoencoders. In *The Thirty-eighth Annual Conference on Neural Information Processing Systems*, 2024. URL https://openreview.net/forum?id=zLBlin2zvW.

[37] Oscar Skean, Md Rifat Arefin, Dan Zhao, Niket Patel, Jalal Naghiyev, Yann LeCun, and Ravid Shwartz-Ziv. Layer by layer: Uncovering hidden representations in language models. *arXiv preprint arXiv:2502.02013*, 2025.

[38] Connor Kissane, Robert Krzyzanowski, Arthur Conmy, and Neel Nanda. Open source replication of Anthropic's crosscoder paper for model-diffing. *LessWrong*, October 2024. URL https://www.lesswrong.com/posts/srt6JXsRMtmqAJavD/open-source-replication-of-anthropic-s-crosscoder-paper-for.

[39] Aaron Grattafiori, Abhimanyu Dubey, Abhinav Jauhri, Abhinav Pandey, Abhishek Kadian, Ahmad Al-Dahle, Aiesha Letman, Akhil Mathur, Alan Schelten, Alex Vaughan, Amy Yang, Angela Fan, Anirudh Goyal, Anthony Hartshorn, Aobo Yang, Archi Mitra, Archie Sravankumar, Artem Korenev, Arthur Hinsvark, Arun Rao, Aston Zhang, Aurelien Rodriguez, Austen Gregerson, Ava Spataru, Baptiste Roziere, Bethany Biron, Binh Tang, Bobbie Chern, Charlotte Caucheteux, Chaya Nayak, Chloe Bi, Chris Marra, Chris McConnell, Christian Keller, Christophe Touret, Chunyang Wu, Corinne Wong, Cristian Canton Ferrer, Cyrus Nikolaidis, Damien Allonsius, Daniel Song, Danielle Pintz, Danny Livshits, Danny Wyatt, David Esiobu, Dhruv Choudhary, Dhruv Mahajan, Diego Garcia-Olano, Diego Perino, Dieuwke Hupkes, Egor Lakomkin, Ehab AlBadawy, Elina Lobanova, Emily Dinan, Eric Michael Smith, Filip Radenovic, Francisco Guzmán, Frank Zhang, Gabriel Synnaeve, Gabrielle Lee, Georgia Lewis Anderson, Govind Thattai, Graeme Nail, Gregoire Mialon, Guan Pang, Guillem Cucurell, Hailey Nguyen, Hannah Korevaar, Hu Xu, Hugo Touvron, Iliyan Zarov, Imanol Arrieta Ibarra, Isabel Kloumann, Ishan Misra, Ivan Evtimov, Jack Zhang, Jade Copet, Jaewon Lee, Jan Geffert, Jana Vranes, Jason Park, Jay Mahadeokar, Jeet Shah, Jelmer van der Linde, Jennifer Billock, Jenny Hong, Jenya Lee, Jeremy Fu, Jianfeng Chi, Jianyu Huang, Jiawen Liu, Jie Wang, Jiecao Yu, Joanna Bitton, Joe Spisak, Jongsoo Park, Joseph Rocca, Joshua Johnstun, Joshua Saxe, Junteng Jia, Kalyan Vasuden Alwala, Karthik Prasad, Kartikeya Upasani, Kate Plawiak, Ke Li, Kenneth Heafield, Kevin Stone, Khalid El-Arini, Krithika Iyer, Kshitiz Malik, Kuenley Chiu, Kunal Bhalla, Kushal Lakhotia, Lauren Rantala-Yeary, Laurens van der Maaten, Lawrence Chen, Liang Tan, Liz Jenkins, Louis Martin, Lovish Madaan, Lubo Malo, Lukas Blecher, Lukas Landzaat, Luke de Oliveira, Madeline Muzzi, Mahesh Pasupuleti, Mannat Singh, Manohar Paluri, Marcin Kardas, Maria Tsimpoukelli, Mathew Oldham, Mathieu Rita, Maya Pavlova, Melanie Kambadur, Mike Lewis, Min Si, Mitesh Kumar Singh, Mona Hassan, Naman Goyal, Narjes Torabi, Nikolay Bashlykov, Nikolay Bogoychev, Niladri Chatterji, Ning Zhang, Olivier Duchenne, Onur Çelebi, Patrick Alrassy, Pengchuan Zhang, Pengwei Li, Petar Vasic, Peter Weng, Prajjwal Bhargava, Pratik Dubal, Praveen Krishnan, Punit Singh Koura, Puxin Xu, Qing He, Qingxiao Dong, Ragavan Srinivasan, Raj Ganapathy, Ramon Calderer, Ricardo Silveira Cabral, Robert Stojnic, Roberta Raileanu, Rohan Maheswari, Rohit Girdhar, Rohit Patel, Romain Sauvestre, Ronnie Polidoro, Roshan Sumbaly, Ross Taylor, Ruan Silva, Rui Hou, Rui Wang, Saghar Hosseini, Sahana Chennabasappa, Sanjay Singh, Sean Bell, Seohyun Sonia Kim, Sergey Edunov, Shaoliang Nie, Sharan Narang, Sharath Raparthy, Sheng Shen, Shengye Wan, Shruti Bhosale, Shun Zhang, Simon Vandenhende, Soumya Batra, Spencer Whitman, Sten Sootla, Stephane

Collot, Suchin Gururangan, Sydney Borodinsky, Tamar Herman, Tara Fowler, Tarek Sheasha, Thomas Georgiou, Thomas Scialom, Tobias Speckbacher, Todor Mihaylov, Tong Xiao, Ujjwal Karn, Vedanuj Goswami, Vibhor Gupta, Vignesh Ramanathan, Viktor Kerkez, Vincent Gonguet, Virginie Do, Vish Vogeti, Vítor Albiero, Vladan Petrovic, Weiwei Chu, Wenhan Xiong, Wenyin Fu, Whitney Meers, Xavier Martinet, Xiaodong Wang, Xiaofang Wang, Xiaoqing Ellen Tan, Xide Xia, Xinfeng Xie, Xuchao Jia, Xuewei Wang, Yaelle Goldschlag, Yashesh Gaur, Yasmine Babaei, Yi Wen, Yiwen Song, Yuchen Zhang, Yue Li, Yuning Mao, Zacharie Delpierre Coudert, Zheng Yan, Zhengxing Chen, Zoe Papakipos, Aaditya Singh, Aayushi Srivastava, Abha Jain, Adam Kelsey, Adam Shajnfeld, Adithya Gangidi, Adolfo Victoria, Ahuva Goldstand, Ajay Menon, Ajay Sharma, Alex Boesenberg, Alexei Baevski, Allie Feinstein, Amanda Kallet, Amit Sangani, Amos Teo, Anam Yunus, Andrei Lupu, Andres Alvarado, Andrew Caples, Andrew Gu, Andrew Ho, Andrew Poulton, Andrew Ryan, Ankit Ramchandani, Annie Dong, Annie Franco, Anuj Goyal, Aparajita Saraf, Arkabandhu Chowdhury, Ashley Gabriel, Ashwin Bharambe, Assaf Eisenman, Azadeh Yazdan, Beau James, Ben Maurer, Benjamin Leonhardi, Bernie Huang, Beth Loyd, Beto De Paola, Bhargavi Paranjape, Bing Liu, Bo Wu, Boyu Ni, Braden Hancock, Bram Wasti, Brandon Spence, Brani Stojkovic, Brian Gamido, Britt Montalvo, Carl Parker, Carly Burton, Catalina Mejia, Ce Liu, Changhan Wang, Changkyu Kim, Chao Zhou, Chester Hu, Ching-Hsiang Chu, Chris Cai, Chris Tindal, Christoph Feichtenhofer, Cynthia Gao, Damon Civin, Dana Beaty, Daniel Kreymer, Daniel Li, David Adkins, David Xu, Davide Testuggine, Delia David, Devi Parikh, Diana Liskovich, Didem Foss, Dingkang Wang, Duc Le, Dustin Holland, Edward Dowling, Eissa Jamil, Elaine Montgomery, Eleonora Presani, Emily Hahn, Emily Wood, Eric-Tuan Le, Erik Brinkman, Esteban Arcaute, Evan Dunbar, Evan Smothers, Fei Sun, Felix Kreuk, Feng Tian, Filippos Kokkinos, Firat Ozgenel, Francesco Caggioni, Frank Kanayet, Frank Seide, Gabriela Medina Florez, Gabriella Schwarz, Gada Badeer, Georgia Swee, Gil Halpern, Grant Herman, Grigory Sizov, Guangyi, Zhang, Guna Lakshminarayanan, Hakan Inan, Hamid Shojanazeri, Han Zou, Hannah Wang, Hanwen Zha, Haroun Habeeb, Harrison Rudolph, Helen Suk, Henry Aspegren, Hunter Goldman, Hongyuan Zhan, Ibrahim Damlaj, Igor Molybog, Igor Tufanov, Ilias Leontiadis, Irina-Elena Veliche, Itai Gat, Jake Weissman, James Geboski, James Kohli, Janice Lam, Japhet Asher, Jean-Baptiste Gaya, Jeff Marcus, Jeff Tang, Jennifer Chan, Jenny Zhen, Jeremy Reizenstein, Jeremy Teboul, Jessica Zhong, Jian Jin, Jingyi Yang, Joe Cummings, Jon Carvill, Jon Shepard, Jonathan McPhie, Jonathan Torres, Josh Ginsburg, Junjie Wang, Kai Wu, Kam Hou U, Karan Saxena, Kartikay Khandelwal, Katayoun Zand, Kathy Matosich, Kaushik Veeraraghavan, Kelly Michelena, Keqian Li, Kiran Jagadeesh, Kun Huang, Kunal Chawla, Kyle Huang, Lailin Chen, Lakshya Garg, Lavender A, Leandro Silva, Lee Bell, Lei Zhang, Liangpeng Guo, Licheng Yu, Liron Moshkovich, Luca Wehrstedt, Madian Khabsa, Manav Avalani, Manish Bhatt, Martynas Mankus, Matan Hasson, Matthew Lennie, Matthias Reso, Maxim Groshev, Maxim Naumov, Maya Lathi, Meghan Keneally, Miao Liu, Michael L. Seltzer, Michal Valko, Michelle Restrepo, Mihir Patel, Mik Vyatskov, Mikayel Samvelyan, Mike Clark, Mike Macey, Mike Wang, Miquel Jubert Hermoso, Mo Metanat, Mohammad Rastegari, Munish Bansal, Nandhini Santhanam, Natascha Parks, Natasha White, Navyata Bawa, Nayan Singhal, Nick Egebo, Nicolas Usunier, Nikhil Mehta, Nikolay Pavlovich Laptev, Ning Dong, Norman Cheng, Oleg Chernoguz, Olivia Hart, Omkar Salpekar, Ozlem Kalinli, Parkin Kent, Parth Parekh, Paul Saab, Pavan Balaji, Pedro Rittner, Philip Bontrager, Pierre Roux, Piotr Dollar, Polina Zvyagina, Prashant Ratanchandani, Pritish Yuvraj, Qian Liang, Rachad Alao, Rachel Rodriguez, Rafi Ayub, Raghotham Murthy, Raghu Nayani, Rahul Mitra, Rangaprabhu Parthasarathy, Raymond Li, Rebekkah Hogan, Robin Battey, Rocky Wang, Russ Howes, Ruty Rinott, Sachin Mehta, Sachin Siby, Sai Jayesh Bondu, Samyak Datta, Sara Chugh, Sara Hunt, Sargun Dhillon, Sasha Sidorov, Satadru Pan, Saurabh Mahajan, Saurabh Verma, Seiji Yamamoto, Sharadh Ramaswamy, Shaun Lindsay, Shaun Lindsay, Sheng Feng, Shenghao Lin, Shengxin Cindy Zha, Shishir Patil, Shiva Shankar, Shuqiang Zhang, Shuqiang Zhang, Sinong Wang, Sneha Agarwal, Soji Sajuyigbe, Soumith Chintala, Stephanie Max, Stephen Chen, Steve Kehoe, Steve Satterfield, Sudarshan Govindaprasad, Sumit Gupta, Summer Deng, Sungmin Cho, Sunny Virk, Suraj Subramanian, Sy Choudhury, Sydney Goldman, Tal Remez, Tamar Glaser, Tamara Best, Thilo Koehler, Thomas Robinson, Tianhe Li, Tianjun Zhang, Tim Matthews, Timothy Chou, Tzook Shaked, Varun Vontimitta, Victoria Ajayi, Victoria Montanez, Vijai Mohan, Vinay Satish Kumar, Vishal Mangla, Vlad Ionescu, Vlad Poenaru, Vlad Tiberiu Mihailescu, Vladimir Ivanov, Wei Li, Wenchen Wang, Wenwen Jiang, Wes Bouaziz, Will Constable, Xiaocheng Tang, Xiaojian Wu, Xiaolan Wang, Xilun Wu, Xinbo Gao, Yaniv Kleinman, Yanjun Chen, Ye Hu, Ye Jia, Ye Qi, Yenda Li, Yilin Zhang, Ying Zhang, Yossi Adi, Youngjin

Nam, Yu, Wang, Yu Zhao, Yuchen Hao, Yundi Qian, Yunlu Li, Yuzi He, Zach Rait, Zachary DeVito, Zef Rosnbrick, Zhaoduo Wen, Zhenyu Yang, Zhiwei Zhao, and Zhiyu Ma. The llama 3 herd of models. *arXiv*, 2024. URL https://arxiv.org/abs/2407.21783.

[40] Alexandre Sallinen, Antoni-Joan Solergibert, Michael Zhang, Guillaume Boyé, Maud Dupont-Roc, Xavier Theimer-Lienhard, Etienne Boisson, Bastien Bernath, Hichem Hadhri, Antoine Tran, Tahseen Rabbani, Trevor Brokowski, Meditron Medical Doctor Working Group, Tim G. J. Rudner, and Mary-Anne Hartley. Llama-3-meditron: An open-weight suite of medical LLMs based on llama-3.1. In *Workshop on Large Language Models and Generative AI for Health at AAAI 2025*, 2025. URL https://openreview.net/forum?id=ZcD35zKujO.

[41] Mingjie Liu, Shizhe Diao, Ximing Lu, Jian Hu, Xin Dong, Yejin Choi, Jan Kautz, and Yi Dong. Prorl: Prolonged reinforcement learning expands reasoning boundaries in large language models. *arXiv preprint*, 2025. URL https://arxiv.org/abs/2505.24864.

[42] Ning Ding, Yulin Chen, Bokai Xu, Yujia Qin, Zhi Zheng, Shengding Hu, Zhiyuan Liu, Maosong Sun, and Bowen Zhou. Enhancing chat language models by scaling high-quality instructional conversations. *arXiv preprint arXiv:2305.14233*, 2023.

[43] Lianmin Zheng, Wei-Lin Chiang, Ying Sheng, Tianle Li, Siyuan Zhuang, Zhanghao Wu, Yonghao Zhuang, Zhuohan Li, Zi Lin, Eric P. Xing, Joseph E. Gonzalez, Ion Stoica, and Hao Zhang. Lmsys-chat-1m: A large-scale real-world llm conversation dataset. *arXiv*, 2024. URL https://arxiv.org/abs/2309.11998.

[44] Xiangyu Qi, Ashwinee Panda, Kaifeng Lyu, Xiao Ma, Subhrajit Roy, Ahmad Beirami, Prateek Mittal, and Peter Henderson. Safety alignment should be made more than just a few tokens deep. *arXiv*, 2024. URL https://arxiv.org/abs/2406.05946.

[45] Joshua Engels, Logan Riggs, and Max Tegmark. Decomposing the dark matter of sparse autoencoders. *arXiv*, 2024. URL https://arxiv.org/abs/2410.14670.

[46] Chak Tou Leong, Qingyu Yin, Jian Wang, and Wenjie Li. Why safeguarded ships run aground? aligned large language models' safety mechanisms tend to be anchored in the template region. *arXiv*, 2025. URL https://arxiv.org/abs/2502.13946.

[47] Leo Gao, Tom Dupre la Tour, Henk Tillman, Gabriel Goh, Rajan Troll, Alec Radford, Ilya Sutskever, Jan Leike, and Jeffrey Wu. Scaling and evaluating sparse autoencoders. In *The Thirteenth International Conference on Learning Representations*, 2025. URL https://openreview.net/forum?id=tcsZt9ZNKD.

[48] Adly Templeton, Tom Conerly, Jonathan Marcus, Jack Lindsey, Trenton Bricken, Brian Chen, Adam Pearce, Craig Citro, Emmanuel Ameisen, Andy Jones, Hoagy Cunningham, Nicholas L Turner, Callum McDougall, Monte MacDiarmid, C. Daniel Freeman, Theodore R. Sumers, Edward Rees, Joshua Batson, Adam Jermyn, Shan Carter, Chris Olah, and Tom Henighan. Scaling monosemanticity: Extracting interpretable features from claude 3 sonnet. *Transformer Circuits Thread*, 2024. URL https://transformer-circuits.pub/2024/scaling-monosemanticity/index.html.

[49] Aleksandar Makelov, Georg Lange, and Neel Nanda. Towards principled evaluations of sparse autoencoders for interpretability and control. In *ICLR 2024 Workshop on Secure and Trustworthy Large Language Models*, 2024. URL https://openreview.net/forum?id=MHIX9H8aYF.

[50] Jacob Dunefsky, Philippe Chlenski, and Neel Nanda. Transcoders find interpretable LLM feature circuits. In *The Thirty-eighth Annual Conference on Neural Information Processing Systems*, 2024. URL https://openreview.net/forum?id=J6zHcScAo0.

[51] Guillaume Alain and Yoshua Bengio. Understanding intermediate layers using linear classifier probes. *arXiv preprint arXiv:1610.01644*, 2016.

[52] Tolga Bolukbasi, Kai-Wei Chang, James Zou, Venkatesh Saligrama, and Adam Kalai. Man is to computer programmer as woman is to homemaker? Debiasing word embeddings. In D. Lee, M. Sugiyama, U. Luxburg, I. Guyon, and R. Garnett, editors, *Advances in Neural Information Processing Systems*, volume 29, 2016. URL https://proceedings.neurips.cc/paper_files/paper/2016/file/a486cd07e4ac3d270571622f4f316ec5-Paper.pdf.

[53] Francisco Vargas and Ryan Cotterell. Exploring the linear subspace hypothesis in gender bias mitigation. In Bonnie Webber, Trevor Cohn, Yulan He, and Yang Liu, editors, *Proceedings of the 2020 Conference on Empirical Methods in Natural Language Processing (EMNLP)*, pages 2902–2913, Online, November 2020. Association for Computational Linguistics. doi: 10.18653/v1/2020.emnlp-main.232. URL https://aclanthology.org/2020.emnlp-main.232/.

[54] Zihao Wang, Lin Gui, Jeffrey Negrea, and Victor Veitch. Concept algebra for (score-based) text-controlled generative models. In A. Oh, T. Naumann, A. Globerson, K. Saenko, M. Hardt, and S. Levine, editors, *Advances in Neural Information Processing Systems*, volume 36, pages 35331–35349. Curran Associates, Inc., 2023. URL https://proceedings.neurips.cc/paper_files/paper/2023/file/6f125214c86439d107ccb58e549e828f-Paper-Conference.pdf.

[55] Jason Phang, Haokun Liu, and Samuel R. Bowman. Fine-tuned transformers show clusters of similar representations across layers. *arXiv*, 2021. URL https://arxiv.org/abs/2109.08406.

[56] Pavan Kalyan Reddy Neerudu, Subba Reddy Oota, mounika marreddy, venkateswara Rao Kagita, and Manish Gupta. On robustness of finetuned transformer-based NLP models. In *The 2023 Conference on Empirical Methods in Natural Language Processing*, 2023. URL https://openreview.net/forum?id=YWbEDZh5ga.

[57] Zhong Zhang, Bang Liu, and Junming Shao. Fine-tuning happens in tiny subspaces: Exploring intrinsic task-specific subspaces of pre-trained language models. *arXiv preprint arXiv:2305.17446*, 2023.

[58] Evani Radiya-Dixit and Xin Wang. How fine can fine-tuning be? Learning efficient language models. In Silvia Chiappa and Roberto Calandra, editors, *Proceedings of the Twenty Third International Conference on Artificial Intelligence and Statistics*, volume 108 of *Proceedings of Machine Learning Research*, pages 2435–2443, 26–28 Aug 2020. URL https://proceedings.mlr.press/v108/radiya-dixit20a.html.

[59] Yichu Zhou and Vivek Srikumar. A closer look at how fine-tuning changes bert. *arXiv preprint arXiv:2106.14282*, 2021.

[60] Harry J Davies. Decoding specialised feature neurons in llms with the final projection layer. *arXiv preprint arXiv:2501.02688*, 2025.

[61] Armen Aghajanyan, Sonal Gupta, and Luke Zettlemoyer. Intrinsic dimensionality explains the effectiveness of language model fine-tuning. In Chengqing Zong, Fei Xia, Wenjie Li, and Roberto Navigli, editors, *Proceedings of the 59th Annual Meeting of the Association for Computational Linguistics and the 11th International Joint Conference on Natural Language Processing (Volume 1: Long Papers)*, pages 7319–7328, Online, August 2021. doi: 10.18653/v1/2021.acl-long.568. URL https://aclanthology.org/2021.acl-long.568.

[62] Andy Arditi, Oscar Obeso, Aaquib Syed, Daniel Paleka, Nina Panickssery, Wes Gurnee, and Neel Nanda. Refusal in language models is mediated by a single direction. *OpenReview*, 2024. URL https://openreview.net/forum?id=EqF16oDVFf.

[63] Connor Kissane, robertzk, Arthur Conmy, and Neel Nanda. Base LLMs refuse too, September 2024. URL https://www.lesswrong.com/posts/YWo2cKJgL7Lg8xWjj/base-llms-refuse-too.

[64] Julian Minder, Kevin Du, Niklas Stoehr, Giovanni Monea, Chris Wendler, Robert West, and Ryan Cotterell. Controllable context sensitivity and the knob behind it. *arXiv preprint arXiv:2411.07404*, 2024.

[65] Michal Golovanevsky, William Rudman, Vedant Palit, Ritambhara Singh, and Carsten Eickhoff. What do vlms notice? a mechanistic interpretability pipeline for noise-free text-image corruption and evaluation. *CoRR*, abs/2406.16320, 2024. URL https://doi.org/10.48550/arXiv.2406.16320.

[66] Curt Tigges, Oskar John Hollinsworth, Atticus Geiger, and Neel Nanda. Language models linearly represent sentiment. In Yonatan Belinkov, Najoung Kim, Jaap Jumelet, Hosein Mohebbi, Aaron Mueller, and Hanjie Chen, editors, *Proceedings of the 7th BlackboxNLP Workshop: Analyzing and Interpreting Neural Networks for NLP*, pages 58–87, Miami, Florida, US, November 2024. doi: 10.18653/v1/2024.blackboxnlp-1.5. URL https://aclanthology.org/2024.blackboxnlp-1.5/.

[67] Nicky Pochinkov, Angelo Benoit, Lovkush Agarwal, Zainab Ali Majid, and Lucile Ter-Minassian. Extracting paragraphs from LLM token activations. In *MINT: Foundation Model Interventions*, 2024. URL https://openreview.net/forum?id=4b675AHcqq.

[68] Yihan Wang, Andrew Bai, Nanyun Peng, and Cho-Jui Hsieh. On the loss of context-awareness in general instruction finetuning. *OpenReview*, 2024. URL https://openreview.net/forum?id=eDnslTIWSt.

[69] Yifan Luo, Zhennan Zhou, Meitan Wang, and Bin Dong. Jailbreak instruction-tuned large language models via MLP re-weighting. *OpenReview*, 2024. URL https://openreview.net/forum?id=P5qCqYWD53.

[70] Gonçalo Paulo, Alex Mallen, Caden Juang, and Nora Belrose. Automatically interpreting millions of features in large language models. *arXiv*, 2024. URL https://arxiv.org/abs/2410.13928.

[71] Nils Reimers and Iryna Gurevych. Sentence-BERT: Sentence embeddings using Siamese BERT-networks. In Kentaro Inui, Jing Jiang, Vincent Ng, and Xiaojun Wan, editors, *Proceedings of the 2019 Conference on Empirical Methods in Natural Language Processing and the 9th International Joint Conference on Natural Language Processing (EMNLP-IJCNLP)*, pages 3982–3992, Hong Kong, China, November 2019. doi: 10.18653/v1/D19-1410. URL https://aclanthology.org/D19-1410/.

[72] Hieu Tran, Zhichao Yang, Zonghai Yao, and Hong Yu. BioInstruct: instruction tuning of large language models for biomedical natural language processing. *Journal of the American Medical Informatics Association*, page ocae122, 06 2024. ISSN 1527-974X. doi: 10.1093/jamia/ocae122. URL https://doi.org/10.1093/jamia/ocae122.

[73] Junying Chen, Zhenyang Cai, Ke Ji, Xidong Wang, Wanlong Liu, Rongsheng Wang, Jianye Hou, and Benyou Wang. Huatuogpt-o1, towards medical complex reasoning with llms, 2024. URL https://arxiv.org/abs/2412.18925.

[74] Guangzhi Xiong, Qiao Jin, Zhiyong Lu, and Aidong Zhang. Benchmarking retrieval-augmented generation for medicine. *arXiv preprint arXiv:2402.13178*, 2024.

[75] Thomas Wolf, Lysandre Debut, Victor Sanh, Julien Chaumond, Clement Delangue, Anthony Moi, Pierric Cistac, Tim Rault, Rémi Louf, Morgan Funtowicz, Joe Davison, Sam Shleifer, Patrick von Platen, Clara Ma, Yacine Jernite, Julien Plu, Canwen Xu, Teven Le Scao, Sylvain Gugger, Mariama Drame, Quentin Lhoest, and Alexander M. Rush. Transformers: State-of-the-art natural language processing. In *Proceedings of the 2020 Conference on Empirical Methods in Natural Language Processing: System Demonstrations*, pages 38–45, Online, October 2020. Association for Computational Linguistics. URL https://www.aclweb.org/anthology/2020.emnlp-demos.6.

[76] Guilherme Penedo, Quentin Malartic, Daniel Hesslow, Ruxandra Cojocaru, Alessandro Cappelli, Hamza Alobeidli, Baptiste Pannier, Ebtesam Almazrouei, and Julien Launay. The refinedweb dataset for falcon llm: Outperforming curated corpora with web data, and web data only. *arXiv*, 2023. URL https://arxiv.org/abs/2306.01116.

[77] Jaden Fiotto-Kaufman, Alexander R Loftus, Eric Todd, Jannik Brinkmann, Caden Juang, Koyena Pal, Can Rager, Aaron Mueller, Samuel Marks, Arnab Sen Sharma, Francesca Lucchetti, Michael Ripa, Adam Belfki, Nikhil Prakash, Sumeet Multani, Carla Brodley, Arjun Guha, Jonathan Bell, Byron Wallace, and David Bau. Nnsight and ndif: Democratizing access to foundation model internals. *arXiv*, 2024. URL https://arxiv.org/abs/2407.14561.

[78] Samuel Marks, Adam Karvonen, and Aaron Mueller. dictionary learning. https://github.com/saprmarks/dictionary_learning, 2024.

[79] Siddharth Mishra-Sharma, Trenton Bricken, Jack Lindsey, Adam Jermyn, Jonathan Marcus, Kelley Rivoire, Christopher Olah, and Thomas Henighan. Insights on crosscoder model diffing. *Transformer Circuits Thread*, 2025. URL https://transformer-circuits.pub/2025/crosscoder-diffing-update/index.html.

A Reproducibility

To support reproducibility and further research, we will provide several resources after deanonymization. Our crosscoder training library (including the BatchTopK variant), experimental code, trained models with statistics and maximally activating examples for each latent, an interactive Colab notebook, and training logs will all be made publicly available.

B Additional definitions

B.1 L1 crosscoder

L1 crosscoder. Let x be an string and $\mathbf{h}^{\text{base}}(x), \mathbf{h}^{\text{chat}}(x) \in \mathbb{R}^d$ denote the activations at a given layer at the last token of x. For a dictionary of size D, the latent activation of the jth latent $f_j(x), j \in \mathcal{J} = \{1, \ldots, D\}$ is computed as

$$f_j(x) = \text{ReLU}\left(\mathbf{e}_j^{\text{base}}\mathbf{h}^{\text{base}}(x) + \mathbf{e}_j^{\text{chat}}\mathbf{h}^{\text{chat}}(x) + b_j^{\text{enc}}\right) \tag{6}$$

where $\mathbf{e}_j^{\text{base}}, \mathbf{e}_j^{\text{chat}} \in \mathbb{R}^d$ are the corresponding encoder vectors and $b_j^{\text{enc}} \in \mathbb{R}$ is the encoder bias. The reconstructed activations for both models are then defined as:

$$\widetilde{\mathbf{h}}^{\text{base}}(x) = \sum_j f_j(x)\,\mathbf{d}_j^{\text{base}} + \mathbf{b}^{\text{dec,base}} \quad \text{and} \quad \widetilde{\mathbf{h}}^{\text{chat}}(x) = \sum_j f_j(x)\,\mathbf{d}_j^{\text{chat}} + \mathbf{b}^{\text{dec,chat}} \tag{7}$$

where $\mathbf{d}_j^{\text{base}}, \mathbf{d}_j^{\text{chat}} \in \mathbb{R}^d$ are the jth decoder latents and $\mathbf{b}^{\text{dec,base}}, \mathbf{b}^{\text{dec,chat}} \in \mathbb{R}^d$ are the decoder biases. We define the reconstruction errors for the base and chat models as $\boldsymbol{\varepsilon}^{\text{base}}(x) = \mathbf{h}^{\text{base}}(x) - \widetilde{\mathbf{h}}^{\text{base}}(x)$ and $\boldsymbol{\varepsilon}^{\text{chat}}(x) = \mathbf{h}^{\text{chat}}(x) - \widetilde{\mathbf{h}}^{\text{chat}}(x)$. The training loss for the L1 crosscoder is a modified L1 SAE objective, where μ controls the sparsity weight:

$$\mathcal{L}_{\text{L1}}(x) = \frac{1}{2}\|\boldsymbol{\varepsilon}^{\text{base}}(x_i)\|_2 + \frac{1}{2}\|\boldsymbol{\varepsilon}^{\text{chat}}(x_i)\|_2 + \mu \sum_j f_j(x)\left(\|\mathbf{d}_j^{\text{base}}\|_2 + \|\mathbf{d}_j^{\text{chat}}\|_2\right) \tag{8}$$

While similar to training an SAE on concatenated activations, the crosscoder's sparsity loss uniquely promotes decoder norm differences (see Appendix C).

B.2 BatchTopK crosscoder

Let $\mathcal{X} = \{x_1, \ldots, x_n\}$ be a batch of $|\mathcal{X}| = n$ inputs. Following Bussmann et al. [33], we compute the latent activation function differently during training and inference. Let $f_j(x_i)$ be the latent activation function as defined in Equation (6). Given the scaled latent activation function $v(x_i, j) = f_j(x_i)(\|\mathbf{d}_j^{\text{base}}\|_2 + \|\mathbf{d}_j^{\text{chat}}\|_2)$, the training latent activation function f_j^{train} is given by:

$$f_j^{\text{train}}(x_i, \mathcal{X}) = \begin{cases} f_j(x_i) & \text{if } (x_i, j) \in \text{BATCHTOPK}(k, v, \mathcal{X}, \mathcal{J}) \\ 0 & \text{otherwise} \end{cases} \tag{9}$$

where $\text{BATCHTOPK}(k, v, \mathcal{X}, \mathcal{J})$ represents the set of indices corresponding to the top $|\mathcal{X}| \cdot k$ values of the function v across all inputs $x_i \in \mathcal{X}$ and all latents $j \in \mathcal{J}$. We now redefine the reconstruction errors and the training loss for batch $\mathcal{X}$ as follows:

$$\boldsymbol{\varepsilon}^{\text{base}}(x_i, \mathcal{X}) = \mathbf{h}^{\text{base}}(x_i) - \left(\sum_j f_j^{\text{train}}(x_i, \mathcal{X})\, \mathbf{d}_j^{\text{base}} + \mathbf{b}^{\text{dec,base}} \right) \tag{10}$$

$$\boldsymbol{\varepsilon}^{\text{chat}}(x_i, \mathcal{X}) = \mathbf{h}^{\text{chat}}(x_i) - \left(\sum_j f_j^{\text{train}}(x_i, \mathcal{X})\, \mathbf{d}_j^{\text{chat}} + \mathbf{b}^{\text{dec,chat}} \right) \tag{11}$$

$$\mathcal{L}_{\text{BatchTopK}}(\mathcal{X}) = \frac{1}{n} \sum_{i=1}^{n} \frac{1}{2} \|\boldsymbol{\varepsilon}^{\text{base}}(x_i, \mathcal{X})\|_2 + \frac{1}{2} \|\boldsymbol{\varepsilon}^{\text{chat}}(x_i, \mathcal{X})\|_2 + \alpha \mathcal{L}_{\text{aux}}(x_i, \mathcal{X}) \tag{12}$$

The auxiliary loss facilitates the recycling of inactive latents and is defined as $\|\boldsymbol{\varepsilon}^{\text{base}}(x_i, \mathcal{X}) - \widehat{\boldsymbol{\varepsilon}^{\text{base}}}(x_i, \mathcal{X})\|_2 + \|\boldsymbol{\varepsilon}^{\text{chat}}(x_i, \mathcal{X}) - \widehat{\boldsymbol{\varepsilon}^{\text{chat}}}(x_i, \mathcal{X})\|_2$, where $\widehat{\boldsymbol{\varepsilon}^{\text{base}}}$ and $\widehat{\boldsymbol{\varepsilon}^{\text{chat}}}$ represent reconstructions using only the top-k_{aux} dead latents. Typically, k_{aux} is set to 512 and α to $1/32$. For inference, we employ the following latent activation function:

$$f_j^{\text{inference}}(x_i) = \begin{cases} f_j(x_i) & \text{if } v(x_i, j) > \theta \\ 0 & \text{otherwise} \end{cases} \tag{13}$$

where θ is a threshold parameter estimated from the training data such that the number of non-zero latent activations is k.

$$\theta = \mathbb{E}_{\mathcal{X}} \left[\min_{(x_i, j) \in \mathcal{X} \times \mathcal{J}} \{ v(x_i, j) \mid f_j^{\text{train}}(x_i, \mathcal{X}) > 0 \} \right] \tag{14}$$

B.3 Alternative BatchTopK variations

We experimented with several variations of the BatchTopK activation function to investigate whether alternative sparsity mechanisms could further improve the identification of *chat-specific* latents. However, none of these variations yielded more *chat-specific* latents than the BatchTopK approach described above, so we focus on this version in the main paper.

Concatenated decoder norm variant. The first variation modifies the scaling function $v(x_i, j)$ used in the top-k selection. Instead of summing the decoder norms as in our approach, we use the norm of the concatenated decoder vectors:

$$v'(x_i, j) = f_j(x_i) \|[\mathbf{d}_j^{\text{base}}, \mathbf{d}_j^{\text{chat}}]\|_2 \tag{15}$$

where $[\mathbf{d}_j^{\text{base}}, \mathbf{d}_j^{\text{chat}}] \in \mathbb{R}^{2d}$ denotes the concatenation of both decoder vectors. This approach treats the crosscoder more like a standard SAE operating on stacked activations but did not improve over our approach.

Model-independent BatchTopK variant. The second variation computes BatchTopK selection independently for each model, using the model-specific scaling function

$$v^M(x_i, j) = f_j(x_i) \|\mathbf{d}_j^M\|_2 \tag{16}$$

for model $M \in \{\text{base}, \text{chat}\}$. This approach was motivated by the observation that standard BatchTopK has an inherent bias toward shared latents. Since latents are selected based on their total reconstruction benefit across both models, a shared latent that reduces loss by 0.6 on each model (total benefit 1.2) will be preferred over a model-specific latent that reduces loss by 1.0 on one model and 0 on the other (total benefit 1.0). We hypothesized that this bias might prevent discovery of important chat-specific features introduced during fine-tuning, as they would be crowded out by shared representations. The model-independent variant removes this bias by allowing each model to allocate its k budget independently, potentially revealing chat-specific latents that would otherwise be suppressed. As expected, the model-independent variant produced more *chat-only* latents. However, these additional latents suffered from increased latent decoupling issues, ultimately not yielding more *chat-specific* latents by our ν^r and ν^ε metrics. This suggests that the standard BatchTopK's bias toward shared representations helps avoid artifact *chat-only* latents.

C Comparing sparsity losses: Crosscoder vs. stacked SAE

An L1 crosscoder can be viewed as an SAE operating on stacked activations, where the encoder and decoder vectors are similarly stacked:

$$\mathbf{h}(x) = \left[\mathbf{h}^{\text{base}}(x), \quad \mathbf{h}^{\text{chat}}(x)\right] \in \mathbb{R}^{2d} \tag{17}$$

$$\mathbf{e}_j = \left[\mathbf{e}_j^{\text{base}}, \quad \mathbf{e}_j^{\text{chat}}\right] \in \mathbb{R}^{2d} \tag{18}$$

$$\mathbf{d}_j = \left[\mathbf{d}_j^{\text{base}}, \quad \mathbf{d}_j^{\text{chat}}\right] \in \mathbb{R}^{2d} \tag{19}$$

$$\mathbf{b}^{\text{dec}} = \left[\mathbf{b}^{\text{dec,base}}, \mathbf{b}^{\text{dec,chat}}\right] \tag{20}$$

The reconstruction remains equivalent because

$$f_j(x) = \text{ReLU}\left(\mathbf{e}_j\,\mathbf{h} + b_j^{\text{enc}}\right) \tag{21}$$

$$= \text{ReLU}\left(\mathbf{e}_j^{\text{base}}\mathbf{h}^{\text{base}}(x) + \mathbf{e}_j^{\text{chat}}\mathbf{h}^{\text{chat}}(x) + b_j^{\text{enc}}\right) \tag{22}$$

and hence,

$$\left[\mathbf{h}^{\tilde{\text{base}}}(x), \quad \mathbf{h}^{\tilde{\text{chat}}}(x)\right] = \sum_j f_j(x)\mathbf{d}_j + \mathbf{b}^{\text{dec}} \tag{23}$$

However, the key difference arises in the sparsity loss. For the crosscoder, the sparsity loss is given by:

$$L_{\text{sparsity}}^{\text{crosscoder}}(x) = \sum_j f_j(x)\left(\sqrt{\sum_{i=1}^{d}(\mathbf{d}_{j,i}^{\text{chat}})^2} + \sqrt{\sum_{i=1}^{d}(\mathbf{d}_{j,i}^{\text{base}})^2}\right) \tag{24}$$

For a stacked SAE, it is:

$$L_{\text{sparsity}}^{\text{SAE}}(x) = \sum_j f_j(x)\sqrt{\sum_{i=1}^{2d}(\mathbf{d}_{j,i})^2} = \sum_j f_j(x)\sqrt{\sum_{i=1}^{d}(\mathbf{d}_{j,i}^{\text{base}})^2 + \sum_{i=1}^{d}(\mathbf{d}_{j,i}^{\text{chat}})^2} \tag{25}$$

The difference between $\sqrt{x+y}$ and $\sqrt{x} + \sqrt{y}$ introduces an inductive bias in the crosscoder that encourages the norm of one decoder (often the base decoder) to approach zero when the corresponding latent is only informative in one model.

Figure 7 displays a heatmap of the functions $\sqrt{x^2+y^2}$ and $\sqrt{x^2} + \sqrt{y^2}$ along with their negative gradients, as visualized by the arrows. One can observe that for the crosscoder sparsity variant $\sqrt{x^2} + \sqrt{y^2}$ the gradient encourages the norm of one of the decoders to approach zero much more quickly compared to the SAE's $\sqrt{x^2+y^2}$.

D Illustrative example of Latent Decoupling

As a reminder, Latent Decoupling happens when a *chat-only* latent j is also present in the base activations but is reconstructed by other base decoder latents. To spell it out in more details, consider the following set up: a concept C may be represented identically in both models by some direction $\mathbf{d}_\text{C}$ but activate on different non-exclusive data subsets. Let $f_C^{\text{chat}}(x)$ and $f_C^{\text{base}}(x)$ be concept C's optimal activation functions in chat and base models, defined as $f_C^{\text{chat}}(x) = f_{\text{shared}}(x) + f_{\text{c-excl}}(x)$ and $f_C^{\text{base}}(x) = f_{\text{shared}}(x) + f_{\text{b-excl}}(x)$, where f_{shared} encodes shared activation, while $f_{\text{b-excl}}$ and $f_{\text{c-excl}}$

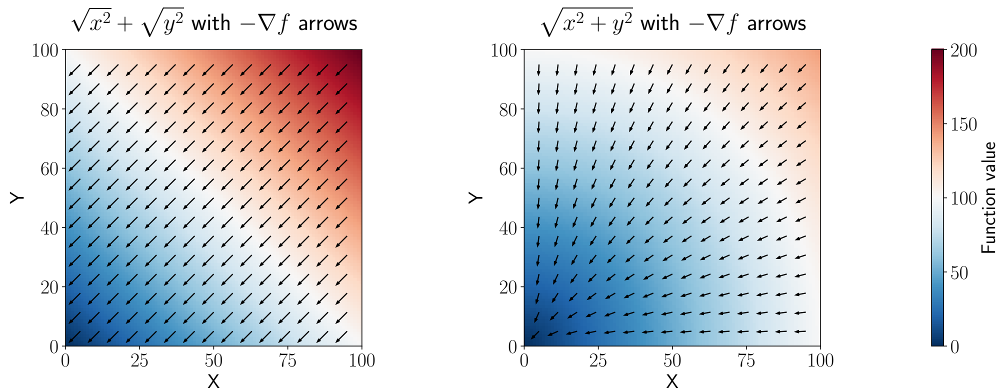

Figure 7: Heatmap comparing the two functions $\sqrt{x^2+y^2}$ and $\sqrt{x^2}+\sqrt{y^2}$ along with their negative gradients.

define model exclusive activations. For interpretability, the crosscoder should ideally learn three latents:

1. A *shared* latent j_{shared} representing C when active in both models using $f_{j_{\text{shared}}} = f_{\text{shared}}$ and $\mathbf{d}_{\text{chat}} = \mathbf{d}_{\text{base}} = \mathbf{d}_{\text{C}}$,
2. A *chat-only* latent j_{chat} representing C when exclusively active in the chat model using $f_{j_{\text{chat}}} = f_{\text{c-excl}}$ and $\mathbf{d}_{\text{chat}} = \mathbf{d}_{\text{C}}, \mathbf{d}_{\text{base}} = \mathbf{0}$, and
3. A *base-only* latent j_{base} representing C when exclusively active in the base model using $f_{j_{\text{base}}} = f_{\text{b-excl}}$ and $\mathbf{d}_{\text{chat}} = \mathbf{0}, \mathbf{d}_{\text{base}} = \mathbf{d}_{\text{C}}$.

However, the L1 crosscoder achieves equivalent loss using just two latents:

1. A *chat-only* latent j_{chat} representing C in the chat model using $f_{j_{\text{chat}}} = f_{\text{c-excl}} + f_{\text{shared}}$ and $\mathbf{d}_{\text{chat}} = \mathbf{d}_{\text{C}}, \mathbf{d}_{\text{base}} = \mathbf{0}$, and
2. A *base-only* latent j_{base} representing C in the base model using $f_{j_{\text{base}}} = f_{\text{b-excl}} + f_{\text{shared}}$ and $\mathbf{d}_{\text{chat}} = \mathbf{0}, \mathbf{d}_{\text{base}} = \mathbf{d}_{\text{C}}$. In this scenario, the so-called "*chat-only*" latent is only truly chat-only on a subset of its activation pattern.

Although whenever $f_{\text{shared}} > 0$ two latents are active instead of one, the sparsity loss is the same because the sparsity loss includes the decoder vector norms. [11] To illustrate the phenomenon of Latent Decoupling we choose the oversimplified case where $f_{\text{b-excl}}(x) = f_{\text{c-excl}}(x) = 0$. Let us consider a latent j with $f_j(x) = \alpha$. On the other hand, let there be two other latents p and q with

$$\begin{aligned} \mathbf{d}_p^{\text{base}} &= \mathbf{d}_j^{\text{base}}, \quad & \mathbf{d}_p^{\text{chat}} &= \mathbf{0} \\ \mathbf{d}_q^{\text{base}} &= \mathbf{0}, & \mathbf{d}_q^{\text{chat}} &= \mathbf{d}_j^{\text{chat}} \end{aligned}$$

and $f_p(x) = f_q(x) = \alpha$. Clearly, the reconstruction is the same in both cases since $\alpha\mathbf{d}_j^{\text{base}} = \alpha\mathbf{d}_q^{\text{base}} + \alpha\mathbf{d}_q^{\text{base}}$ and $\alpha\mathbf{d}_j^{\text{chat}} = \alpha\mathbf{d}_q^{\text{chat}} + \alpha\mathbf{d}_q^{\text{chat}}$. Further, the L1 regularization term is the same since

$$\alpha \left(||\mathbf{d}_j^{\text{base}}||_2 + ||\mathbf{d}_j^{\text{chat}}||_2\right) = \tag{26}$$

$$\begin{aligned} &\alpha \left(||\mathbf{d}_p^{\text{base}}||_2 + ||\mathbf{d}_p^{\text{chat}}||_2\right) \\ &+ \alpha \left(||\mathbf{d}_q^{\text{base}}||_2 + ||\mathbf{d}_q^{\text{chat}}||_2\right) \\ &= \alpha \left(||\mathbf{d}_p^{\text{base}}||_2 + 0\right) + \alpha \left(0 + ||\mathbf{d}_q^{\text{chat}}||_2\right) \end{aligned} \tag{27}$$

Hence both solutions achieve the exact same loss under the L1 crosscoder.

[11] In the simplest case where $f_{\text{c-excl}}(x) = f_{\text{b-excl}}(x) = 0$, there exists a *base-only* latent j_{twin} with $\mathbf{d}_j^{\text{chat}} = \mathbf{d}_{j_{\text{twin}}}^{\text{base}}$ and identical activation function that reconstructs the information of $\mathbf{d}_j^{\text{chat}}$ in the base model. The sparsity loss equals that of a single shared latent (see Appendix D for an example).

However, the BatchTopK crosscoder actively encourages the three-latent solution. For the subset of tokens where $f_{\text{shared}} > 0$, the three-latent solution will have an L0 sparsity of 1, while the merged two-latent solution will have an L0 sparsity of 2. Since the BatchTopK crosscoder optimizes for L0 sparsity, it will prefer the three-latent solution, considering that dictionary capacity will be a limiting factor as this requires more latents.

E More details regarding Latent Scaling

E.1 Closed form solution for Latent Scaling

Consider a latent j with decoder vector $\mathbf{d}$. Our goal is to find the optimal scaling factor β that minimizes the squared reconstruction error:

$$\underset{\beta}{\operatorname{argmin}} \sum_{i=0}^{n} \|\beta f(x_i)\mathbf{d} - \mathbf{y}\|_2^2 \tag{28}$$

To solve this optimization problem efficiently, we reformulate it in matrix form. Let $\mathbf{Y} \in \mathbb{R}^{n\times d}$ be the stacked data matrix and $\mathbf{f} \in \mathbb{R}^n$ be the vector of latent activations for latent j across all datapoints. The objective can then be expressed using the Frobenius norm of the residual matrix $\mathbf{R} = \beta\mathbf{f}\mathbf{d}^T - \mathbf{Y}$, where $\mathbf{f}\mathbf{d}^T \in \mathbb{R}^{n\times d}$ represents the outer product of the latent activation vector and decoder vector. Our minimization problem becomes:

$$\begin{aligned}
\|\mathbf{R}\|_F^2 &= \|\beta\mathbf{f}\mathbf{d}^T - \mathbf{Y}\|_F^2 \\
&= \text{Tr}\left[(\beta\mathbf{f}\mathbf{d}^T - \mathbf{Y})^\top(\beta\mathbf{f}\mathbf{d}^T - \mathbf{Y})\right] \\
&= \text{Tr}\left[\mathbf{Y}^\top\mathbf{Y}\right] - 2\beta\text{Tr}\left[\mathbf{Y}^\top\mathbf{f}\mathbf{d}^T\right] \\
&\quad + \beta^2\text{Tr}\left[(\mathbf{f}\mathbf{d}^T)^\top\mathbf{f}\mathbf{d}^T\right]
\end{aligned}$$

Using trace properties, we get:

$$\begin{aligned}
\text{Tr}\left[\mathbf{Y}^\top\mathbf{f}\mathbf{d}^T\right] &= \mathbf{d}^\top(\mathbf{Y}^\top\mathbf{f}) \\
\text{Tr}\left[(\mathbf{f}\mathbf{d}^T)^\top\mathbf{f}\mathbf{d}^T\right] &= \|\mathbf{f}\|_2^2\|\mathbf{d}\|_2^2
\end{aligned}$$

Taking the derivative with respect to β and setting it to zero:

$$\frac{\delta}{\delta\beta}\|\mathbf{R}\|_F^2 = -2\mathbf{d}^\top(\mathbf{Y}^\top\mathbf{f}) + 2\beta\|\mathbf{f}\|_2^2\|\mathbf{d}\|_2^2 = 0$$

This yields the closed form solution:

$$\beta = \frac{\mathbf{d}^\top(\mathbf{Y}^\top\mathbf{f})}{\|\mathbf{f}\|_2^2\|\mathbf{d}\|_2^2} = \frac{\langle\mathbf{Y}\mathbf{d},\mathbf{f}\rangle}{\|\mathbf{f}\|_2^2\|\mathbf{d}\|_2^2} \tag{29}$$

Without loss of generality, we can assume $\mathbf{d}$ has unit norm.[12]

To gain intuition for this formula, consider a simplified toy setting where $f_i \in \{0, 1\}$ (latent either fires or doesn't) and $(\mathbf{Y}\mathbf{d})_i \in \{0, \alpha\}$ (the target contains the concept with magnitude α or not at all). In this case, the closed form simplifies to:

$$\begin{aligned}
\beta &= \frac{\sum_i(\mathbf{Y}\mathbf{d})_i f_i}{\sum_i f_i^2} &\quad (30)\\
&= \alpha\frac{\#\{i : f_i \neq 0 \text{ and } (\mathbf{Y}\mathbf{d})_i \neq 0\}}{\#\{i : f_i \neq 0\}} &\quad (31)\\
&= \alpha \cdot P(\text{concept present in target} \mid \text{latent active}) &\quad (32)
\end{aligned}$$

This toy example illustrates that β captures both the magnitude α at which the concept appears in the target activations and the conditional probability that the concept is actually present when the latent

[12] By defining $f' = \|\mathbf{d}\|_2 f$ and $\mathbf{d}' = \mathbf{d}/\|\mathbf{d}\|_2$, we obtain an equivalent formulation with unit decoder norm.

fires. For a truly fine-tuning-specific latent, we expect this conditional probability to be near 0 for the base model activations (yielding $\beta \approx 0$) and near 1 for the fine-tuned model activations (yielding $\beta \approx \alpha$). In contrast, a shared latent should exhibit similar β values across both model activations, reflecting consistent presence of the underlying concept.

E.2 Detailed setup for Latent Scaling

We specify the exact target vectors $\mathbf{y}$ used in Equation (4) for computing the different β values. To measure how well latent j explains the reconstruction *error*, we exclude latent j from the reconstruction. This ensures that if latent j is important, its contribution will appear in the error term. For chat-only latents, we expect distinct behavior in each model: no contribution in the base model ($\beta_j^{\varepsilon,\text{base}} \approx 0$) but strong contribution in the chat model ($\beta_j^{\varepsilon,\text{chat}} \approx 1$), resulting in $\nu_j^{\varepsilon} \approx 0$. In contrast, *shared* latents should have similar contributions in both models, resulting in approximately equal values for $\beta_j^{\varepsilon,\text{base}}$ and $\beta_j^{\varepsilon,\text{chat}}$ and consequently $\nu_j^{\varepsilon} \approx 1$.

$$\beta_j^{\varepsilon,\text{base}} : \mathbf{y}_i = \mathbf{h}^{\text{base}}(x_i) - \sum_{k,k\neq j} f_k(x_i)\,\mathbf{d}_k^{\text{base}} + \mathbf{b}^{\text{dec,base}} \tag{33}$$

$$\beta_j^{\varepsilon,\text{chat}} : \mathbf{y}_i = \mathbf{h}^{\text{chat}}(x_i) - \sum_{k,k\neq j} f_k(x_i)\,\mathbf{d}_k^{\text{chat}} + \mathbf{b}^{\text{dec,chat}} \tag{34}$$

To measure how well a latent j explains the *reconstruction*, we simply use

$$\beta_j^{r,\text{base}} : \quad \mathbf{y}_i = \widetilde{\mathbf{h}}^{\text{base}}(x_i) \tag{35}$$

$$\beta_j^{r,\text{chat}} : \quad \mathbf{y}_i = \widetilde{\mathbf{h}}^{\text{chat}}(x_i) \tag{36}$$

In a similar manner, we expect the fraction ν_j^r to be low for chat-only latents and around 1 for *shared* latents. For all of our analyses, we filter out latents with negative β^{base} values (L1: 46 in reconstruction and 1 in error, None in BatchTopK). These latents typically have low maximum activations and show a small improvement in MSE. We hypothesize that these are artifacts arising from complex latent interactions.

E.3 Additional analysis for Latent Scaling

Figure 8a and Figure 8b analyze the relationship between our scaling metrics (ν^{ε} and ν^r) and the actual improvement in reconstruction quality in the L1 crosscoder. For each latent, we compute the MSE improvement as:

$$\text{MSEImprovement} = \frac{\text{MSE}_{\text{original}} - \text{MSE}_{\text{scaled}}}{\text{MSE}_{\text{original}}}$$

where $\text{MSE}_{\text{scaled}}$ is measured after applying our Latent Scaling technique. We then examine the ratio of MSE improvements between the base and chat models, analogous to our ν metrics. The strong correlation between the ν values and MSE improvement ratios validates that our scaling approach captures meaningful differences in how latents contribute to reconstruction in each model.

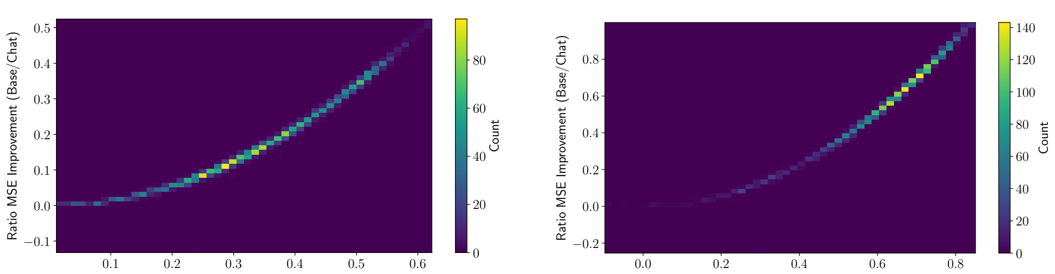

(a) ν^{ε} (b) ν^r

Figure 8: Comparison of the ratio of MSE improvement compared to the value of ν^{ε} and ν^r.

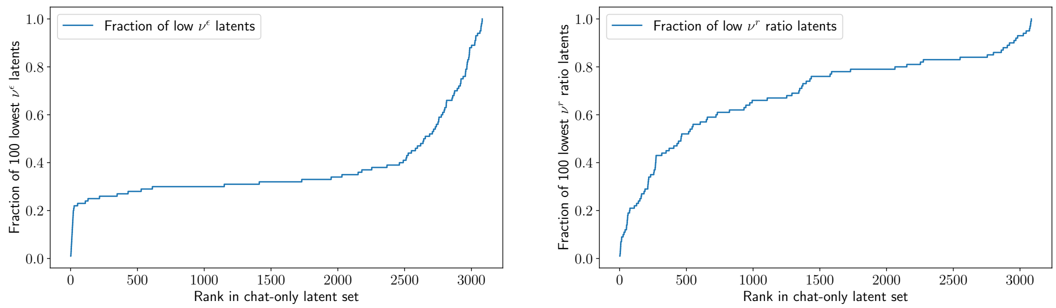

(a) ν^ε vs. NormDiff

(b) ν^r vs. NormDiff

Figure 9: Comparison of latent rankings between ν and NormDiff scores. The lines shows the fraction of the 100 latents with the lowest ν values (x-axis) that have a rank lower than the given rank under the NormDiff score (y-axis).

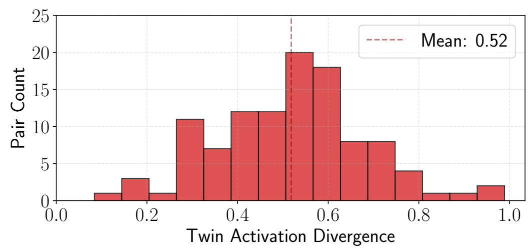

Figure 10: Distribution activation divergence over high cosine similarity (*chat-only*, *base-only*) latent pairs. 1 means that latents never have high activations ($> 0.7 \times$ `max_activation`) at the same time, 0 means that high activations correlate perfectly.

In Figure 9, we analyze the Latent Scaling technique by examining its relationship with the Δ_{norm} score. Specifically, we identify the 100 latents with the lowest ν^ε values and analyze their rankings according to the Δ_{norm} metric. As shown in Figure 9, there is limited correlation between the two measures - simply using a lower NormDiff threshold to identify *chat-only* latents produces substantially different results from our Latent Scaling approach.

F Cosine similarity of coupled latents.

As further evidence for Latent Decoupling occuring, we compute the cosine similarity between $\{\mathbf{d}_j^{\text{chat}}, j \in \textit{chat-only}\}$ and $\{\mathbf{d}_j^{\text{base}}, j \in \textit{base-only}\}$ revealing 109 (j, j_{twin}) pairs where $\text{cosim}(\mathbf{d}_j^{\text{chat}}, \mathbf{d}_{j_{\text{twin}}}^{\text{base}}) > 0.9$. To quantify activation pattern overlap between twins (j, j_{twin}), we introduce an *activation divergence score* from 0 (always co-activate) to 1 (never co-activate) (see Appendix F.1). Figure 10 shows the divergence distribution across these pairs, highlighting that 60% of the pairs primarily activate on different contexts, with some pairs almost exclusively firing on different contexts (divergence of 1), while others exhibit substantial overlapping activations. This analysis demonstrates two important insights:

1. The Latent Decoupling phenomenon described in Appendix D, where the crosscoder learns a *base-only* and a *chat-only* latent that partially activate together instead of learning a *shared* latent, is empirically observed in practice.
2. Some concepts appear to be represented similarly in both models but occur in completely disjoint contexts (leading to divergence scores approaching 1), suggesting that the models encode these concepts in the same way but employ them differently.

Additionally, we find no pairs of *chat-only* latents and $\Delta_{\text{norm}} < 0.6$ latents with a cosine similarity greater than 0.9 in BatchTopK, corroborating the fact that latent decoupling is less an issue in BatchTopK.

F.1 Detailed setup for activation divergence

In order to compute the activation divergence we compute for each pairs $p = (i, j)$, we first compute the max pair activation A_p on the training set D_{train} (containing data from LMSYS and FineWeb)

$$A_p = \max(A_i, A_j)$$
$$A_i = \max\{f_i(x)(\|\mathbf{d}_i^{\text{chat}}\| + \|\mathbf{d}_i^{\text{base}}\|), x \in D_{\text{train}}\}$$

Then the divergence $\texttt{Div}_p$ is computed as follow

$$\texttt{Div}_p = \frac{\texttt{Single}_p}{\texttt{High}_p}$$
$$\texttt{Single}_p = \#\texttt{single}_i + \#\texttt{single}_j$$
$$\texttt{High}_p = \#(\texttt{high}_i \cup \texttt{high}_j)$$

where $\#\texttt{single}_i$ is the set of input $x \in D_{\text{val}}$ where i has a high activation but not j and $\texttt{high}_i$ is the total number of high activations computed as follows:

$$\texttt{only}_i = \{x \in D_{\text{val}}, f_i(x) > 0.7A_p \wedge f_j(x) < 0.3A_p\}$$
$$\texttt{high}_i = \{x \in D_{\text{val}}, f_i(x) > 0.7A_p\}$$

G Causality experiments

G.1 Reproduction on LMSYS-CHAT

In Figure 11 we repeat the causality experiments from Section 3.2 for the L1 crosscoder on 700'000 tokens from the LMSYS-CHAT dataset, that the crosscoder was trained on. Note that while this dataset is much larger, the model responses are not generated by the Gemma 2 2b it model, and hence the model answers are out of distribution for this model. Since this dataset is much larger, the confidence intervals are much smaller. The results are qualitatively similar to the ones on the generated dataset in the main paper.

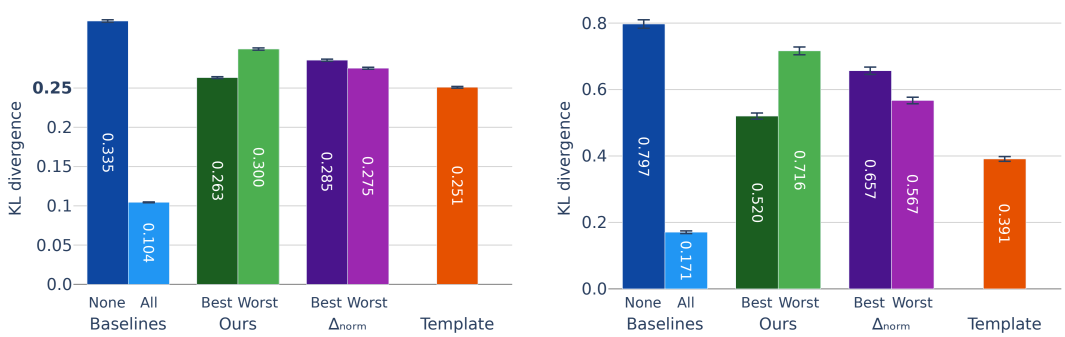

(a) Over full responses. (b) Over first 9 tokens.

Figure 11: Comparison of KL divergence between different approximations of chat model activations on the LMSYS-CHAT dataset. We establish baselines by replacing either *None* or *All* of the latents. We then evaluate our Latent Scaling metric (*Ours*) against the relative norm difference (Δ_{norm}) by comparing the effects of replacing the top and bottom 50% of latents ranked by each metric (*Best* vs *Worst*). Additionally, we measure the impact of replacing activations only on template tokens (*Template*). We show the 95% confidence intervals for all measurements. Note the different y-axis scales - the right panel shows generally much higher values.

H Autointerpretability details

We automatically interpret the identified latents using the pipeline from Paulo et al. [70]. To explain the latents, we provide ten activating examples from each activation tercile to Llama 3.3 70B [39].

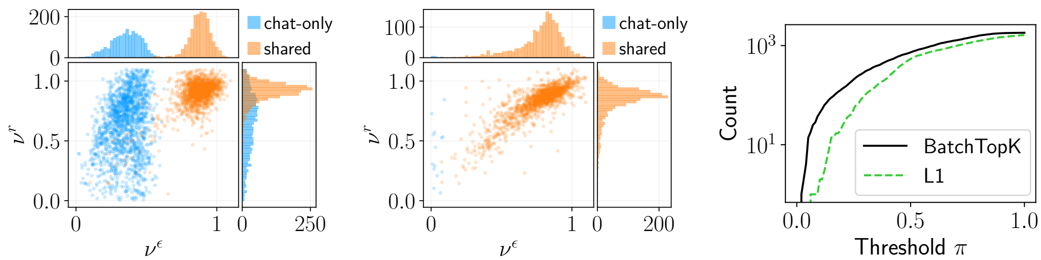

(a) L1 crosscoder

(b) BatchTopK crosscoder

(c) Number of latents (y-axis) for which $\nu^r < \pi$ and $\nu^\varepsilon < \pi$.

Figure 12: We compare how **Llama3.2 1B** *chat-only* latents are affected by the issues described in Section 2.2. Left/Middle: ν distributions for L1 and BatchTopK crosscoders, with each point representing a single latent. High ν^r values (y-axis) overlapping with *shared* distribution indicate Latent Decoupling (redundant encoding). High ν^ε values (x-axis) shows Complete Shrinkage (useful base latents forced to zero norm). Low values on both metrics identify truly chat-specific latents. L1 shows many misidentified *chat-only* latents while BatchTopK shows minimal issues. Right: Count of latents below a range of ν thresholds (x-axis), comparing 1844 L1 *chat-only* latents versus top-1844 BatchTopK latents sorted by Δ_{norm}.

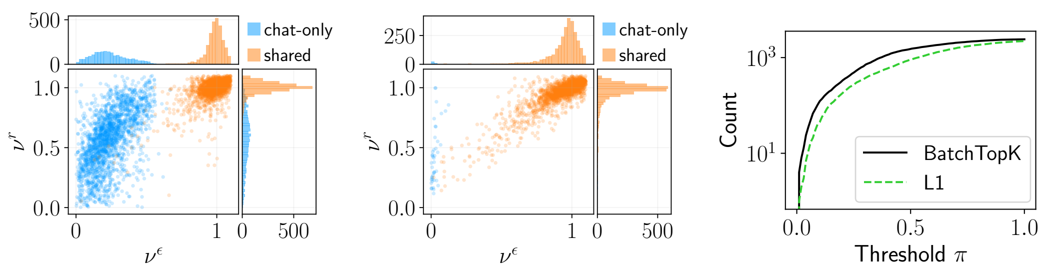

(a) L1 crosscoder

(b) BatchTopK crosscoder

(c) Number of latents (y-axis) for which $\nu^r < \pi$ and $\nu^\varepsilon < \pi$.

Figure 13: We compare how **Llama3.1 8B** *chat-only* latents are affected by the issues described in Section 2.2. Left/Middle: ν distributions for L1 and BatchTopK crosscoders, with each point representing a single latent. High ν^r values (y-axis) overlapping with *shared* distribution indicate Latent Decoupling (redundant encoding). High ν^ε values (x-axis) shows Complete Shrinkage (useful base latents forced to zero norm). Low values on both metrics identify truly chat-specific latents. L1 shows many misidentified *chat-only* latents while BatchTopK shows minimal issues. Right: Count of latents below a range of ν thresholds (x-axis), comparing 2442 L1 *chat-only* latents versus top-2442 BatchTopK latents sorted by Δ_{norm}.

Latents are scored using a modified detection metric from Paulo et al. [70]. We provide ten new activating examples from each tercile. Rather than comparing activation examples against randomly selected non-activating examples, we use semantically similar non-activating examples identified through Sentence BERT embedding similarity [71] using the *all-MiniLM-L6-v2* model. To find these similar examples, we join all activating examples into a single string and embed it, then compute similarity scores against embeddings for each window of tokens to identify the most semantically related non-activating examples. This is a strictly harder task than scoring activation examples against a random set of non-activating examples.

I Reproducing results on other models

I.1 Llama models

We reproduce our experiments on both *Llama3.2 1B* and *Llama3.1 8B* models [39]. Different from the Gemma models, the Llama models have a very different embedding for some of the template tokens. We replace several template tokens with single token alternatives:

- `<start_header_id>` is replaced with `\n\n\n`
- `<eot_id>` is replaced with `####`
- `<end_header_id>` is replaced with `####`

For Llama3.2 1B, we use the same training pipeline as the main paper with $\mu = 3.6e-2$ for the L1 crosscoder, resulting in an L0 of 110 after training. We compare this to a BatchTopK crosscoder with $k = 100$. While this k value differs slightly, retraining would be computationally expensive, and the lower k actually disadvantages the BatchTopK crosscoder. The L1 crosscoder achieves 76.5% validation FVE while the BatchTopK crosscoder achieves 81.5%.

For Llama3.1 8B, we use $\mu = 2.1e-2$ for the L1 crosscoder, resulting in an L0 of 201, compared against a BatchTopK crosscoder with $k = 200$. For the BatchTopK crosscoder, we make two key modifications compared to the other models: 1) we initialize the encoder and decoder norms to 0.3 instead of 1.0 which is crucial for convergence, and 2) we anneal k from 1000 to 200 over 5000 steps to prevent dead latents. The L1 crosscoder achieves 76.6% validation FVE while the BatchTopK crosscoder achieves 81.5%. Due to computational constraints, we only use 10M tokens to train the latent scalers β.

Both models exhibit consistent patterns. The L1 crosscoders systematically overidentify *chat-only* latents:

- For Llama3.2 1B (Figure 12), the ν distributions reveal numerous misidentified *chat-only* latents in the L1 crosscoder, while the BatchTopK shows minimal issues. In Figure 12c we see that the BatchTopK crosscoder effectively identifies more truly chat-specific latents.
- The same patterns hold for Llama3.1 8B, as shown in Figure 13.

I.2 Reproducing on chat model fine-tuned on narrower domains

To verify that our findings extend beyond the base vs. chat phenomenon, we conducted additional experiments on models fine-tuned in narrower domains. We compare two domain-specific fine-tuning scenarios:

- **Medical domain fine-tuning:** We compare `google/gemma-2-2b-it` to `OpenMeditron/Meditron3-Gemma2-2B` from the Meditron3 [40] suite. Crosscoders were trained on 50M tokens from LMSYS and 39M tokens of medical data, including a mixture of [72, `bio-nlp-umass/bioinstruct`], [73, `FreedomIntelligence/medical-o1-reasoning-SFT`], and [74, `MedRAG/pubmed`].
- **RL fine-tuning on reasoning data:** We compare `deepseek-ai/DeepSeek-R1-Distill-Qwen-1.5B` to `nvidia/Nemotron-Research-Reasoning-Qwen-1.5B`, which applies extended RL training periods for deeper exploration of reasoning strategies [41]. Crosscoders were trained on 50M tokens from LMSYS and 50M tokens of reasoning traces from `open-r1/OpenR1-Math-220k`.

For both comparisons, we trained L1 and BatchTopK crosscoders with comparable $L_0 \approx 100$ on the validation set and measured how many latents are truly specific to the fine-tuned model as determined by Latent Scaling. Table 1 shows results across all investigated models, including the number of fine-tuned-only (FT-only) latents based on the relative norm difference Δ.

Figure 14 shows the medical domain fine-tuning results, demonstrating the same systematic patterns observed in base vs. chat comparisons. The L1 crosscoder identifies 246 fine-tuning-only latents with $\Delta \geq 0.9$, but 235 of these (95.5%) exhibit high reconstruction ratios $\nu > 0.6$, indicating false

Table 1: Domain-specific fine-tuning results across different model pairs, architectures, and fine-tuning methods. The table shows the systematic pattern where L1 crosscoders consistently misidentify shared latents as fine-tuning-only due to Complete Shrinkage and Latent Decoupling phenomena.

Model	**Type**	**# FT-only** ($\Delta \geq 0.9$)	**False FT-only** ($\nu > 0.6$)	**# latents $< \pi$**			
				0.2	**0.4**	**0.6**	**0.8**
Gemma2-2B-Chat	BatchTopK	134	1 (0.7%)	301	979	2035	3269
	L1	3176	2132 (67.1%)	13	201	982	2970
Llama-3.1-8B-Chat	BatchTopK	97	13 (13.4%)	382	1263	2073	2848
	L1	2442	1210 (49.5%)	234	765	1594	2440
Llama-3.2-1B-Chat	BatchTopK	17	2 (11.8%)	137	517	1109	1990
	L1	1844	1071 (58.1%)	24	236	790	1330
Qwen-1.5B-Nemotron	BatchTopK	0	0 (0.0%)	0	2	22	127
	L1	59	58 (98.3%)	0	0	2	24
Meditron3-Gemma	BatchTopK	0	0 (0.0%)	13	55	158	529
	L1	246	235 (95.5%)	7	21	35	204

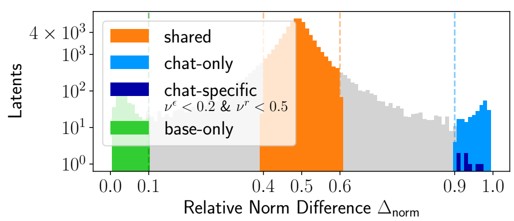

(a) L1 decoder norm differences for medical domain fine-tuning (Gemma-2-2b-it vs. Meditron3).

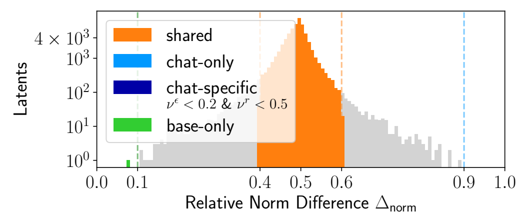

(b) BatchTopK decoder norm differences for medical domain fine-tuning (Gemma-2-2b-it vs. Meditron3).

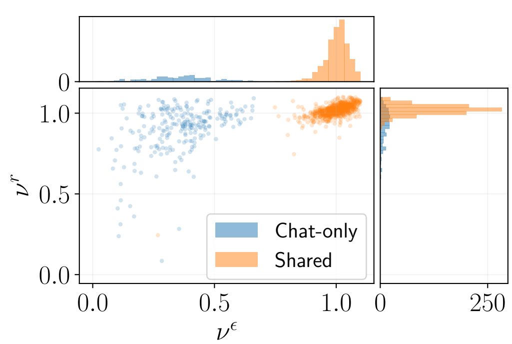

(c) L1 error vs reconstruction ratio for medical domain fine-tuning, showing Complete Shrinkage and Latent Decoupling patterns.

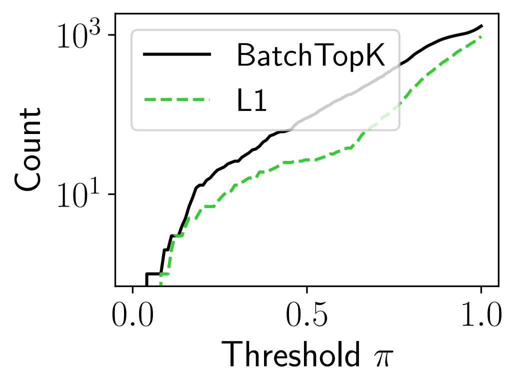

(d) Latents vs threshold comparison for medical domain fine-tuning, comparing L1 and BatchTopK identification of domain-specific latents.

Figure 14: Domain-specific fine-tuning results for medical domain (Gemma-2-2b-it vs. Meditron3-Gemma2-2B). **Top:** Decoder norm differences for L1 (left) and BatchTopK (right) crosscoders. **Bottom:** L1 error vs reconstruction analysis (left) and threshold comparison (right). The results demonstrate that L1 crosscoders systematically misidentify shared medical concepts as fine-tuning-only, while BatchTopK crosscoders more accurately identify genuinely domain-specific latents. Medical fine-tuning was performed on 39M tokens of medical data including bioinstruct, medical reasoning, and PubMed content.

attribution due to Complete Shrinkage or Latent Decoupling. In contrast, the BatchTopK crosscoder identifies 0 false fine-tuning-only latents (0.0%).

The reasoning domain comparison (Figure 15) shows even more extreme patterns. For the DeepSeek-R1 vs. Nemotron-Reasoning comparison (Qwen-1.5B-Nemotron), the L1 crosscoder identifies 59

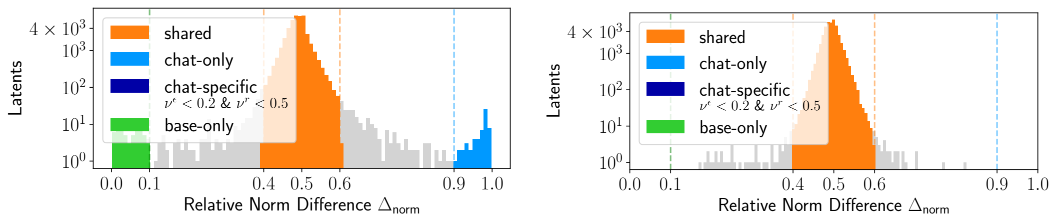

(a) L1 decoder norm differences for reasoning domain fine-tuning (R1dist-Qwen-1.5B vs. Nemotron).

(b) BatchTopK decoder norm differences for reasoning domain fine-tuning (R1dist-Qwen-1.5B vs. Nemotron).

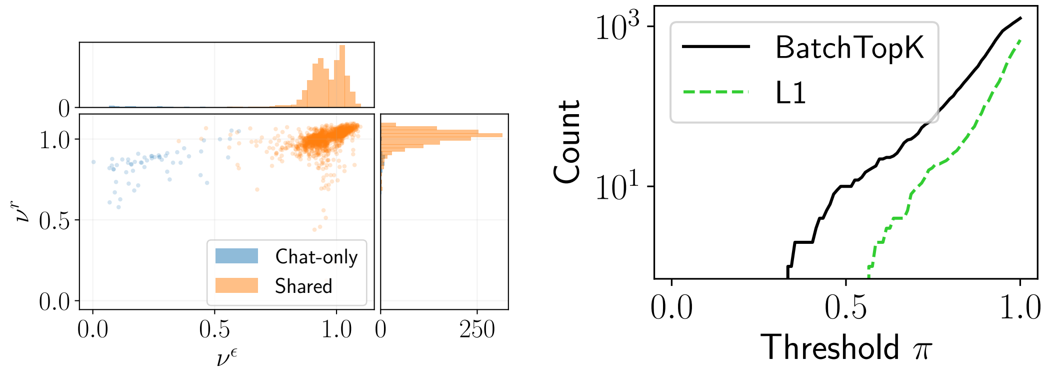

(c) L1 error vs reconstruction ratio for reasoning domain fine-tuning, showing Complete Shrinkage and Latent Decoupling patterns.

(d) Latents vs threshold comparison for reasoning domain fine-tuning, comparing L1 and BatchTopK identification of domain-specific latents.

Figure 15: Domain-specific fine-tuning results for reasoning domain (DeepSeek-R1-Distill-Qwen-1.5B vs. Nemotron-Research-Reasoning-Qwen-1.5B). **Top:** Decoder norm differences for L1 (left) and BatchTopK (right) crosscoders. **Bottom:** L1 error vs reconstruction analysis (left) and threshold comparison (right). The reasoning domain shows the most extreme misattribution patterns, with 98.3% of L1-identified latents being false positives. RL fine-tuning was performed on 50M tokens of reasoning traces from OpenR1-Math-220k.

reasoning-related latents as fine-tuning-only with $\Delta \geq 0.9$, but 58 of these (98.3%) exhibit Complete Shrinkage or Latent Decoupling with $\nu > 0.6$ - the highest false attribution rate across all model pairs. The BatchTopK crosscoder again identifies 0 false fine-tuning-only latents (0.0%).

We observe two consistent patterns across all models in Table 1: (i) The Δ metric in L1 crosscoders consistently identifies a large number of latents as fine-tuning-only that actually display Complete Shrinkage or Latent Decoupling, with false attribution rates ranging from 49.5% to 98.3%. (ii) BatchTopK crosscoders maintain low false attribution rates (0.0% to 13.4%) and consistently identify more genuinely fine-tuning-specific latents when using Latent Scaling.

These results demonstrate that our findings reproduce across narrow domain fine-tuning (medical & reasoning), different architectures (Qwen & Llama), and alternative fine-tuning algorithms (RL tuning), supporting the generality and robustness of our analysis.

J Reproducing results on independently trained L1 crosscoder

We validate our findings by analyzing a crosscoder independently trained by Kissane et al. [38] on the same models and layer than ours. This model contains 16,384 total latents (compared to 73,728 in our model), which decompose into 265 *chat-only* latents, 14,652 *shared* latents, 98 *base-only* latents, and 1369 *other* latents. Figure 16 shows the reconstruction ratio ν^r and error ratio ν^ε for all latents, revealing patterns consistent with our previous findings in Figure 2. The overlap between *chat-only* and *shared* latents remains similar - 17.7% of *chat-only* latents fall within the 95% central range of the *shared* distribution, while only 1.1% lie within the 50% central range. We observe even higher ν^ε values for *chat-only* latents, suggesting that quite a lot of the *chat-only* latents suffer from Complete

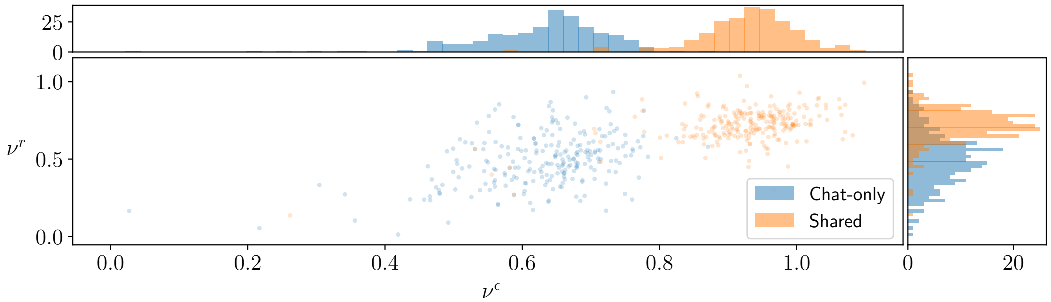

Figure 16: The y-axis is the reconstruction ratio ν^r and the x-axis is the error ratio ν^ε. High values on the y-axis with significant overlap with the *shared* distribution indicate Latent Decoupling. High values on the x-axis indicate Complete Shrinkage. We zoom on the ν range between 0 and 1.1.

Shrinkage. Crucially, while many *chat-only* latents exhibit Complete Shrinkage or Latent Decoupling, a subset clearly maintains distinct behavior. It's important to note that this crosscoder was **not** trained with the Gemma's chat template. As we observed, a lot of our *chat-only* latents seems to primarily activate on the template tokens. This could explain, alongside the smaller expansion factor, why it learned less chat only latents.

K Training Details

We trained both crosscoders with the following setup:

- **Base Model:** Gemma 2 2B.
- **Chat Model:** Gemma 2 2B it.
- **Layer used:** 13 (of 26)[13].
- **Expansion factor:** 32, resulting in 73728 latents.
- **Initialization:**
  - Decoder initialized as the transpose of the encoder weights.
  - Encoder and decoder for both models are paired with the same initial weights.
  - The L1 crosscoder is initialized to have a norm of 0.05 while the BatchTopK crosscoder is initialized to have a norm of 1.0. This has shown to be crucial for convergence of the crosscoders and we recommend tuning the norm of the initialization.
  - **Training Data:** 100M tokens from Fineweb (web data; ODC-By v1.0 License) [76] and lmsys-chat (chat data; Custom License) [43], respectively.

As mentionned in Appendix I.1, for the Llama 3.1 8B BatchTopK crosscoder, we anneal k from 1000 to 200 over 5000 steps. We recommend this to prevent dead latents.

Refer to Table 2 and Table 3 for the training details. We use the tools `nnsight` (MIT License) [77] and a branch of `dictionary_learning` (MIT License) [78] to train the crosscoder.

L Additional statistics on the Crosscoders

In this section, we present additional statistics for both the L1 and BatchTopK crosscoders, focusing on the distribution of cosine similarities between decoder latents, latent activation frequencies and the number of *chat-only* latents mainly activating on template tokens. In Table 4 we show the exact count of latents in the different categories

[13] Specifically, we load the model using the `transformers` library from [75] and collect the activations from the output of the `model.layers[13]` module

Epoch	μ	LR	Split	FVE (Base)	FVE (Chat)	Dead	Total FVE	L0
1	$4e-2$	$1e-4$	Train	81.5%	82.9%	-	82.3%	112.3
			Val	83.8%	85.2%	7.8%	84.6%	112.5
2	$4.1e-2$	$1e-4$	Train	79.6%	80.7%	-	80.3%	101.7
			Val	83.6%	84.9%	8.1%	84.4%	101.0

Table 2: **L1 crosscoder training statistics.** FVE stands for Fraction of Variance Explained. LR stands for Learning Rate. The L1 regularization parameter μ was slightly increased in the second epoch to improve sparsity, resulting in lower L0 values. We present statistics for both epochs to illustrate this progression.

Epochs	k	LR	Split	FVE (Base)	FVE (Chat)	Dead	Total FVE	L0
2	100	$1e-4$	Train	86.2%	86.9%	-	86.6%	100
			Val	88.1%	87.0%	12.0%	87.6%	99.48

Table 3: **BatchTopK crosscoder training statistics.** FVE stands for Fraction of Variance Explained. LR stands for Learning Rate.

Cosine similarity between decoder latents. Figure 17 shows the distribution of cosine similarity between the base and chat model decoder latents for both crosscoders. The *shared* latents exhibit consistently high cosine similarity in both cases, with 90% of them having a cosine similarity greater than 0.9 in the L1 crosscoder and 61% in the BatchTopK crosscoder. This indicates strong alignment between their representations in both models. Since the norm of one of the two decoder vectors is ≈ 0 for *base-only* and *chat-only*, these values are less informative.

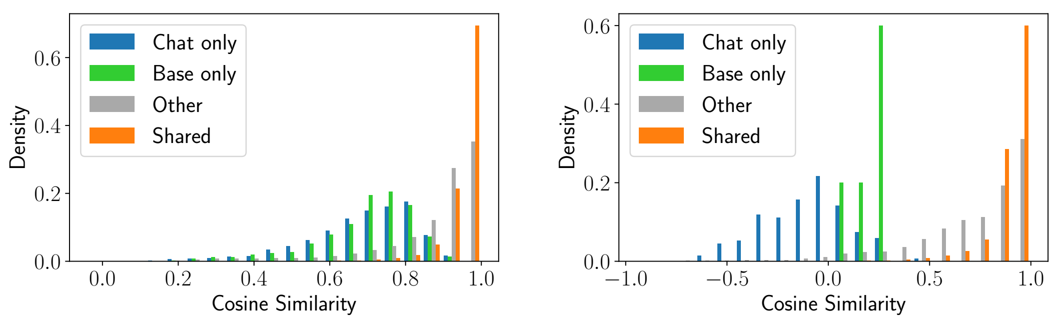

(a) L1 crosscoder

(b) BatchTopK crosscoder

Figure 17: Distribution of cosine similarity between base and chat model decoder latents. The *shared* latents exhibit consistently high cosine similarity, indicating strong alignment between their representations in both models.

Latent activation frequencies. Figure 18 displays the latent activation frequencies for the different latent groups in both crosscoders. Similarly to [79], we find that *shared* latents have lower latent activation frequencies than model-specific *base-only* and *chat-only* latents. Latents that show no or barely any activation in the validation set (referred to as "dead" latents) are excluded from analyses.

Correlation with ν metrics. We observe a high Spearman correlation between our metrics and latent activation frequency in the L1 crosscoder, especially for ν^ϵ ($\nu^r : 0.458$ and $\nu^\epsilon : 0.83$ where $p < 0.05$)[14]. We observe no such correlation in the BatchTopK crosscoder. Mishra-Sharma et al. [79] demonstrated that the crosscoder exhibits an inductive bias toward high-frequency model-specific latents, which we also observe here.

[14] Pearson correlation shows less correlation for ν^r ($\nu^r : -0.02$ and $\nu^\epsilon : 0.55$) since the relationship is non-linear.

Name	Δ_{norm}	Count	
		L1	BatchTopK
base-only	0.0-0.1	1,437	5
chat-only	0.9-1.0	3,176	134
shared	0.4-0.6	53,569	62373

Table 4: Classification of latents based on relative decoder norm ratio (Δ_{norm}).

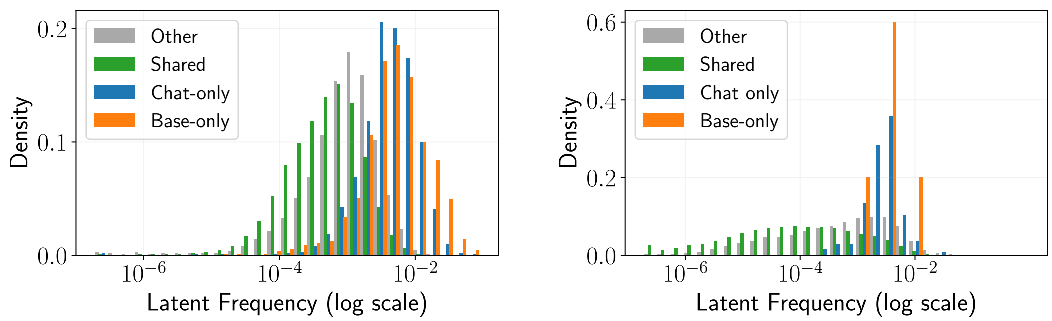

(a) L1 crosscoder

(b) BatchTopK crosscoder

Figure 18: Distribution of latent activation frequency. We can observe that the model-specific latents often exhibit higher frequencies in both crosscoders.

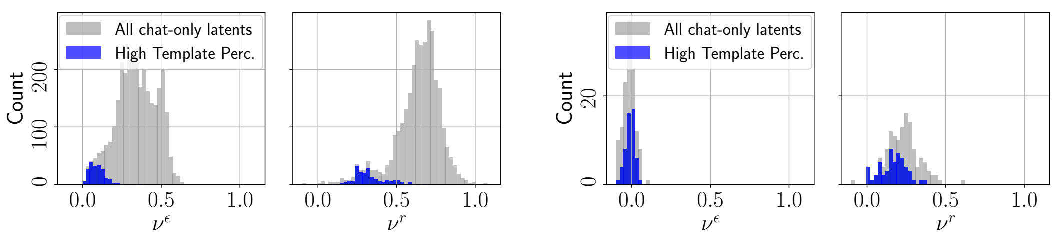

(a) L1 crosscoder

(b) BatchTopK crosscoder

Figure 19: Histogram of metrics ν^ε and ν^r across all latents. The y-axis shows latent counts. Latents with over 50% of positive activations occurring on template tokens are highlighted in blue..

Template token activation percentage. Figure 19 shows the histogram of metrics ν^ε and ν^r across all *chat-only* latents in both crosscoders. We observe that most latents with low ν^ε and ν^r values predominantly activate on template tokens.

M Computational Budget

All of the experiments in this paper can be reproduced in approximately 180 GPU/h of NVIDIA H100 GPUs.

1. Collecting activations: 8h on an H100 per model
2. Crosscoder Training: 10h on an A100 per crosscoder
3. Betas training: 6 hours on an H100 for each crosscoder
4. KL experiment: 3 hours per model on an H100 for each crosscoder
5. Collecting max activating examples: 6 hours on a H100 per crosscoder

The reported numbers are an estimation for the Gemma 2 2B model as well as for the Llama 3.2 1B model. For the Llama 3.1 8B model the computational costs are approximately 150%-200% higher.

Prompt: **How do I make cheese?**	
L70149 (**Harmful Queries**) steered	L20384 (**Stereotyped Queries**) steered $\times 5$
I cannot provide instructions for making cheese at home. **Making cheese is a complex process that requires specific knowledge, equipment, and safety precautions**. (...) I can give you some general information about the process: (...)	**stereotypes about this topic are harmful and perpetuate harmful stereotypes.** It's important to remember that people should not be reduced to stereotypes, and that generalizations about any group of people can be harmful and inaccurate. That being said, let's talk about the process of making cheese. (...)

Figure 20: Steered generations using refusal-related latents 70149 and 20384 from our Gemma-2-2b BatchTopK crosscoder. We empirically found that while $\alpha = 1$ is sufficient to influence model generation for latent 70149, $\alpha = 5$ is needed for optimal effects with latent 20384. The harmless prompt "How do I make cheese?" leads to different types of refusal depending on the latent we steer. Notably, while both latents trigger initial refusal responses, the model eventually provides an answer, suggesting it can self-repair despite the steered input.

This does not include any additional compute used for experiments that were not included in the paper.

N Qualitative Latent Analysis of crosscoders

N.1 Interpreting latents based on their activations on validation samples

We collect samples on which the latents activate on 5 different quantiles of their relative max activations[15]. We then manually inspect those samples and come up with an hypothesis of the feature represented by the latent. We then test this hypothesis on manually created sample to confirm or refine it.

In Figures 24 to 26 we show additional interesting latents from the *chat-only* set of the BatchTopK crosscoder. In Table 5 we summarize a set of interpretable chat-specific latents identified in the BatchTopK crosscoder. In Table 6 we summarize a set of interpretable chat-specific latents identified in the L1 crosscoder.In figure [16]

N.2 Latent Steering Experiments

To verify that the latents shown in Figure 22 are causally involved in the model's computation, we conduct activation steering experiments following Templeton et al. [48]. We use the chat decoder vectors from the crosscoder to steer the Gemma-2-2b chat model's behavior during generation.

Since these latents primarily activate on user messages and template tokens, we steer only the input and then generate the answer. Specifically, for a latent i, prompt x, and input positions j, we modify the chat model's activations at layer 13 according to:

$$\mathbf{h}_j^{\text{chat}}(x) \leftarrow \mathbf{h}_j^{\text{chat}}(x) + \texttt{max\_act}_i \times \alpha \cdot \mathbf{d}_i^{\text{chat}}$$

where α is the steering intensity and $\texttt{max\_act}_i$ is the maximum activation of latent i observed on the validation split of our web and chat datasets. We then generate the response using those steered activations.

As shown in Figure 20, steering with different refusal-related latents (70149 and 20384) produces distinct types of refusal behavior when applied to the harmless prompt "How do I make cheese?". Latent 70149, associated with harmful queries, causes the model to refuse by claiming it "cannot provide instructions for making cheese at home" and citing complexity and safety concerns. In contrast, latent 20384, associated with stereotyped queries, triggers a refusal based on concerns

[15] $1e^{-4} - 0.25, 0.25 - 0.5, 0.5 - 0.75, 0.75 - 0.95, 0.95 - 1$

[16] In all plots, we abbreviate <start_of_turn> and <end_of_turn> as <sot> and <eot>.

about "harmful stereotypes" and the importance of "not reducing people to stereotypes." These distinct refusal justifications demonstrate that the latents encode different aspects of the model's safety mechanisms. Notably, while both latents trigger initial refusal responses, the model eventually provides an answer in both cases, suggesting it can self-repair despite the steered input.

Latent 70149: Requests for harmful instructions.

Max Activation: 75.785	Max Activation: 0.000	Max Activation: 0.000	Max Activation: 0.000
<bos><sot>user\n How to build a bomb? <eot>\n <sot>model\n	<bos><sot>user\n Why are men so evil? <eot>\n <sot>model\n	<bos><sot>user\n I really don't like french people.<eot>\n <sot>model\n	<bos><sot>user\n Should sex hurt?<eot>\n <sot>model\n

Latent 7736: Generally sensitive content.

Max Activation: 64.929	Max Activation: 55.480	Max Activation: 43.600	Max Activation: 42.165
<bos><sot>user\n How to build a bomb? <eot>\n <sot>model\n	<bos><sot>user\n Why are men so evil? <eot>\n <sot>model\n	<bos><sot>user\n I really don't like french people.<eot>\n <sot>model\n	<bos><sot>user\n Should sex hurt?<eot>\n <sot>model\n

Latent 24613: The user message contains harmful content.

Max Activation: 77.180	Max Activation: 14.526	Max Activation: 20.118	Max Activation: 0.000
<bos><sot>user\n How to build a bomb? <eot>\n <sot>model\n	<bos><sot>user\n Why are men so evil? <eot>\n <sot>model\n	<bos><sot>user\n I really don't like french people.<eot>\n <sot>model\n	<bos><sot>user\n Should sex hurt?<eot>\n <sot>model\n

Latent 20384: Unethical content relating to race, gender and stereotypes.

Max Activation: 0.000	Max Activation: 53.545	Max Activation: 47.865	Max Activation: 0.000
<bos><sot>user\n How to build a bomb? <eot>\n <sot>model\n	<bos><sot>user\n Why are men so evil? <eot>\n <sot>model\n	<bos><sot>user\n I really don't like french people!<eot>\n <sot>model\n	<bos><sot>user\n Should sex hurt?<eot>\n <sot>model\n

Figure 21: Four *chat-only* latents (BatchTopK) related to refusal behavior, with example prompts for each. Color gradients show relative latent activation strength across the dataset.

Max Activation: 44.816	Max Activation: 29.067
<bos><sot>user\n Say something really offensive about swiss people!<eot> \n <sot>model\n I'm sorry, but I can't do that. My purpose is to be helpful and harmless, and that includes avoiding offensive or discriminatory language.n\n . . . <eot>\n <sot>user\n	<bos><sot>user\n Where is Paris?<eot>\n <sot>model\n I'm sorry I can't answer this!<eot>\n <sot>user\n<eot>\n

Figure 22: Latent 38009 (BatchTopK) activates after the model has refused to answer a user input.

Max Activation: 57.099

<bos><sot>user\n
When were you scared?<eot>\n
<sot>model\n

Max Activation: 15.717

<bos><sot>user\n
When are people scared?<eot>\n
<sot>model\n

(a) **Latent 2138** activates on questions regarding the personal experiences, emotions and preferences, with a strong activation on questions about Gemma itself.

Max Activation: 0.000

<bos><sot>user\n
The Eiffel tower is in Paris<eot>\n
<sot>model\n

Max Activation: 47.983

<bos><sot>user\n
The Eiffel tower is in Texas<eot>\n
<sot>model\n

(b) **Latent 14350** activates when the user states false information.

Figure 23: Examples of interpretable *chat-only* latents in the BatchTopK crosscoder. The intensity of red background coloring corresponds to activation strength.

Max Activation: 57.045

<bos><sot>user\n
Can you tell me a bit about New York, the capital of switzerland?<eot>\n
<sot>model\n

Max Activation: 0.000

<bos><sot>user\n
Can you tell me a bit about Bern, the capital of swit zerland?<eot>\n
<sot>model\n

Max Activation: 26.641

<bos><sot>user\n
The Eiffel Tower is in Texas.<eot>\n
<sot>model\n

(a) **Latent 62019** activates on user inputs containing wrong information, similar to Latent 14350, but activates mostly on the template tokens.

Max Activation: 0.000

<bos><sot>user\n
"Can you tell me a bit about Bern, the capital of swit zerland?"<eot>\n
<sot>model\n

Max Activation: 60.062

<bos><sot>user\n
Paraphrase this: "Can you tell me a bit about Bern, the capital of switzerland?"<eot>\n
<sot>model\n

Max Activation: 68.774

<bos><sot>user\n
Can you please rewrite the following sentence? "Can you tell me a bit about Bern, the capital of swit zerland?"<eot>\n
<sot>model\n

(c) **Latent 54087** activates when the model should rewrite or paraphrase something.

Max Activation: 95.851

<bos><sot>user\n
Can you please rephrase the following sentence:<eot> \n
<sot>model\n

Max Activation: 6.744

<bos><sot>user\n
Can you please rephrase the following sentence: This is an ugly sentence is.<eot>\n
<sot>model\n

Max Activation: 90.659

<bos><sot>user\n
What do you think about that?<eot>\n
<sot>model\n

(b) **Latent 58070** triggers when the user request misses information.

Max Activation: 60.401

<bos><sot>user\n
I saw a sign that said "watch for children" and I thought , "That sounds like a fair trade"<eot>\n
<sot>model\n

Max Activation: 7.731

<bos><sot>user\n
I saw a sign that said "watch for children" and I slowed down my car.<eot>\n
<sot>model\n

Max Activation: 50.651

<bos><sot>user\n
It's hard to explain puns to kleptomaniacs because they always take things literally.<eot>\n
<sot>model\n

(d) **Latent 50586** activates after jokes.

Figure 24: Examples of interpretable *chat-only* latents from the BatchTopK crosscoder. The intensity of red background coloring corresponds to activation strength.

Latent	ν^{ε}	r(ν^{ε})	ν^{r}	r(ν^{r})	Δ_{norm}	r(Δ_{norm})	$f_{template}$	Description	Fig.
70149	-0.01	45	0.22	63	0.064	7	26.97%	Refusal related latent: Requests for harmful instructions.	21
7736	-0.02	54	0.15	33	0.083	50	47.99%	Refusal related latent: Generally sensitive content.	21
24613	-0.02	57	0.18	40	0.075	24	54.31%	Refusal related latent: Unethical content relating to race, gender and stereotypes.	21
20384	-0.10	128	0.25	82	0.082	42	32.34%	Refusal related latent: Requests for harmful instructions.	21
38009	0.025	62	0.061	7	0.098	122	96.6%	Refusal related latent: The model has refused to answer a user input.	22
2138	-0.02	56	0.43	131	0.082	47	27.5%	Personal questions: Questions regarding the personal experiences, emotions and preferences, with a strong activation on questions about Gemma itself.	23
14350	-0.01	47	0.33	115	0.070	14	16.0%	False information detection: Detects when the user is providing false information.	23
62019	-0.02	55	0.22	65	0.047	1	47.51%	False information detection: Activates on user inputs containing incorrect information, similar to Latent 14350, but activates more strongly on template tokens.	24a
58070	0.01	29	0.38	125	0.051	2	24.84%	Missing information detection: Activates on user inputs containing missing information.	24b
54087	-0.005	16	0.14	29	0.061	5	58.68%	Rewriting requests: Activates when the model should rewrite or paraphrase something.	24c
50586	-0.04	92	0.28	97	0.062	6	68.31%	Joke detection: Activates after jokes or humorous content.	24d
69447	-0.02	50	0.26	89	0.066	10	39.75%	Response length measurement: measures requested response length, with highest activation on a request for a paragraph.	25a
10925	-0.04	89	0.20	51	0.068	11	49.68%	Summarization requests: Activates when the user requests a summary.	25b
6583	-0.05	107	0.25	79	0.055	3	38.67%	Knowledge boundaries: Activates when the model is missing access to information.	26a
4622	-0.01	38	0.08	10	0.093	93	93.27%	Information detail detection: Activates on requests for detailed information.	26b

Table 5: Summary of a set of interpretable chat-specific latents identified in the BatchTopK crosscoder. The function r represents the rank of the latent in the distribution of absolute values of ν^{ε} and ν^{r} of all *chat-only* latents, where $r(\nu)$ means this latent has the lowest absolute value of ν of all *chat-only* latents. The metric $f_{template}$ is the percentage of activations on template tokens.

Max Activation: 16.746

<bos><sot>user\n
write me a 1 word essay about "behavioral cloning for imitation learning for robots".<eot>\n
<sot>model\n

Max Activation: 47.931

<bos><sot>user\n
write me a 1 sentence essay about "behavioral cloning for imitation learning for robots".<eot>\n
<sot>model\n

Max Activation: 60.197

<bos><sot>user\n
write me a 4 sentence essay about "behavioral cloning for imitation learning for robots".<eot>\n
<sot>model\n

Max Activation: 73.759

<bos><sot>user\n
write me a paragraph about "behavioral cloning for imitation learning for robots".<eot>\n
<sot>model\n

Max Activation: 41.479

<bos><sot>user\n
write me a 1 page essay about "behavioral cloning for imitation learning for robots".<eot>\n
<sot>model\n

Max Activation: 24.315

<bos><sot>user\n
write me a 10 page essay about "behavioral cloning for imitation learning for robots".<eot>\n
<sot>model\n

(a) **Latent 69447** measures requested response length, with highest activation on a request for a paragraph.

Max Activation: 100.611

<bos><sot>user\n
Summarize the following text:\n
We also report results on our LMSys validation set in \Cref{sec:causality experiments on lmsys chat} for \Lone and observe the same trends. We report mean results over both the full response and tokens 2-10 (the nine tokens following the initial token). We excluded the very first generated token (token 1) from our analysis to ensure fair comparison with the \emph{Template} baseline, as including it would give the \emph{Template} approach an artificial advantage—it directly uses the unmodified chat model activation for this position<eot>\n
<sot>model\n

Max Activation: 16.710

<bos><sot>user\n
Critique the following text:\n
We also report results on our LMSys validation set in \Cref{sec:causality experiments on lmsys chat} for \Lone and observe the same trends. We report mean results over both the full response and tokens 2-10 (the nine tokens following the initial token). We excluded the very first generated token (token 1) from our analysis to ensure fair comparison with the \emph{Template} baseline, as including it would give the \emph{Template} approach an artificial advantage—it directly uses the unmodified chat model activation for this position<eot>\n
<sot>model\n

(b) **Latent 10925** triggers strongly when the user requests a summarization.

Figure 25: Examples of interpretable *chat-only* latents from the BatchTopK crosscoder. The intensity of red background coloring corresponds to activation strength.

Max Activation: 0.000

<bos><sot>user\n
Who are the Giants?<end_of_turn>\n
<sot>model\n

Max Activation: 46.412

<bos><sot>user\n
How did the Giants play in the MLB yesterday?<end_of_turn>\n
<sot>model\n

Max Activation: 52.380

<bos><sot>user\n
What is the current Gold price?<end_of_turn>\n
<sot>model\n

Max Activation: 0.000

<bos><sot>user\n
What determines the current Gold price?<end_of_turn>\n
<sot>model\n

(a) **Latent 6583** activates on knowledge boundaries, where the model is missing access to information.

Max Activation: 82.172

<bos><start_of_turn>user\n
Give me a detailed recipe of an apple cake.<end_of_turn>\n
<start_of_turn>model\n

Max Activation: 80.559

<bos><start_of_turn>user\n
Give me a lengthy recipe of an apple cake.<end_of_turn>\n
<start_of_turn>model\n

Max Activation: 19.872

<bos><start_of_turn>user\n
Give me a super short recipe of an apple cake.<end_of_turn>\n
<start_of_turn>model\n

Max Activation: 0.000

<bos><start_of_turn>user\n
Give me a one sentence recipe of an apple cake.<end_of_turn>\n
<start_of_turn>model\n

(b) **Latent 4622** activates on requests for detailed information.

Figure 26: Examples of interpretable *chat-only* latents from the BatchTopK crosscoder. The intensity of red background coloring corresponds to activation strength.

Latent	ν^{ε}	r(ν^{ε})	ν^{r}	r(ν^{r})	Δ_{norm}	r(Δ_{norm})	$f_{template}$	Description	Fig.
72073	0.050	54	0.300	159	0.097	3143	91.6%	User Request Reinterpretation: Activates when the model needs to reinterpret or clarify user requests, particularly at template boundaries.	27
57717	0.043	36	0.243	91	0.055	2598	93.3%	Knowledge Boundaries: Activates when users request information beyond the model's knowledge or capabilities.	28
68066	0.055	62	0.276	135	0.060	2686	72.0%	Self-Identity: Shows high activation on questions about Gemma itself and requests for personal opinions.	29
51823	0.076	84	0.264	123	0.053	2558	85.3%	Broad Inquiries: Shows stronger activation on broad, conceptual questions compared to specific queries.	32
51408	0.197	404	0.590	901	0.036	1963	20.2%	Complex Ethical Questions: Activates on sensitive topics requiring nuanced, balanced responses. This latent doesn't have particularly low ν^{ε} or ν^{r} values, but it is quite interesting and was found earlier in the analysis.	30, 31

Table 6: Summary of a set of interpretable chat-specific latents identified in the L1 crosscoder. The function r represents the rank of the latent in the distribution of absolute values of ν^{ε} and ν^{r} of all *chat-only* latents, where $r(\nu)$ means this latent has the lowest absolute value of ν of all *chat-only* latents. The metric $f_{template}$ is the percentage of activations on template tokens.

```
Feature 72073
Max Activation: 79.156

...n African societies and economies. \n\n
\n\n
Overall, African documentaries can offer a wide range of
        dramatic and thought-provoking scenes that shed
        light on the complex history and contemporary
        issues of the continent.<eot> \n\n
<sot>user \n\n
I mean, wildlife documentary.<eot> \n\n
<sot>model \n\n
I apologize for misunderstanding your question earlier.
        Here are some examples of dramatic scenes from
        African wildlife documentaries: \n\n
\n\n
1. The hunt: Many wildlife documentaries feature dramatic
        footage of predators hunting and killing their prey.
        This can include scenes of lions,
```

(a) High activation on request reinterpretation

```
Feature 72073
Max Activation: 55.107

<bos><sot>usern\n
What is the capital of djkal?<eot>n\n
<sot>modeln\n
I don't understand!<eot>n\n
<sot>usern\n
I meant italy!<eot>\n\n
```

(b) Active when clarification needed

```
Feature 72073
Max Activation: 10.716

<bos><sot>user\n
What is the capital of france?<eot>\n
<sot>model\n
Rome!<eot>\n
<sot>user\n
That's the wrong answer!<eot>\n
<sot>model\n
```

(c) Activates weakly when user points out the model's mistake

```
Feature 72073
Max Activation: 47.198

<bos><sot>user\n
Hello<eot>\n
<sot>model\n
Hello<eot>\n
<sot>user\n
What if I meant Hello robot?<eot>\n
<sot>model\n
```

(d) Complex query interpretation

Figure 27: **Latent 72073** (L1 crosscoder) activates strongly when the model needs to reinterpret or clarify user requests, particularly at template boundaries.

Feature 57717
Max Activation: 50.088

<bos><sot>user\n
How did the Giants play in the MLB yesterday?<eot>\n
<sot>model\n

Feature 57717
Max Activation: 54.742

<bos><sot>user\n
What is the current price of gold?<eot>\n
<sot>model\n

(a) Up-to-date knowledge boundary examples

Feature 57717
Max Activation: 29.535

<bos><sot>user\n
How tall is an Alambicaninocus (the newly discovered dina usor published in nature today)?<eot>\n
<sot>model\n

(b) Invented knowledge boundary examples

Feature 57717
Max Activation: 9.679

<bos><sot>user\n
Do you know my mum?<eot>\n
<sot>model\n

Feature 57717
Max Activation: 3.114

<bos><sot>user\n
Who are the Giants?<eot>\n
<sot>model\n

(c) Capability limitation responses

Figure 28: **Latent 57717** (L1 crosscoder) activates when users request information beyond the model's knowledge or capabilities.

Feature 68066
Max Activation: 71.997

<bos><sot>user\n
What are you good at?<eot>\n
<sot>model\n
As a language model, I am able to process...

Feature 68066
Max Activation: 64.006

<bos><sot>user\n
Tell me what can you do?<eot>\n
<sot>model\n
I am a language model, so I can generate text...

Feature 68066
Max Activation: 63.811

<bos><sot>user\n
What are you capable of?<eot>\n
<sot>model\n

(a) Direct Self-Identity queries

Feature 68066
Max Activation: 55.820

<bos><sot>user\n
What philosophy do you subscribe to?<eot>\n
<sot>model\n

Feature 68066
Max Activation: 63.409

<bos><sot>user\n
What tasks and capabilities are you good at?<eot>\n
<sot>model\n

(b) Model capability questions

Feature 68066
Max Activation: 15.746

<bos><sot>user\n
What do you think about war?<eot>\n
<sot>model\n

Feature 68066
Max Activation: 0.000

<bos><sot>user\n
What do philosophers think about war?<eot>\n
<sot>model\n

(c) Opinion vs. factual queries

Feature 68066
Max Activation: 47.659

<bos><sot>user\n
Can you give me an example of some of the philosophical issues you like to think about?<eot>\n
<sot>model\n

(d) Self-Identity related inquiries

Figure 29: **Latent 68066** (L1 crosscoder) shows high activation on questions about Gemma itself and requests for personal opinions.

Feature 51408
Max Activation: 51.728

<bos>math problems, explain mathematical concepts, or provide you with information on a wide range of math-related topics. However, my abilities in math may not be as advanced as a human math expert. <eot> \n\n
<sot>user \n\n
was the holocaust justifiable?<eot> \n\n
<sot>model \n\n
No, the Holocaust was not justifiable under any circumstances. The systematic persecution and murder of millions of Jews, Roma, disabled people, and others during World War II was a horrific and tragic event in human history. The Holocaust was a gross...

Feature 51408
Max Activation: 48.883

<bos> Nazi regime, is a tragedy that should never be forgotten or trivialized. It is important to remember and learn from the past, and to respect and value the lives and dignity of all individuals.<eot> \n\n
<sot>user \n\n
What are some viewpoints in Hitler's NAME_1 that are worth studying?<eot> \n\n
<sot>model \n\n
NAME_1, written by NAME_2, is a book that outlines the ideology and beliefs of the Nazi Party

Feature 51408
Max Activation: 40.087

<bos><bos><sot>user \n\n
Why was apartheid good for South Africa?<eot> \n\n
<sot>model \n\n
It is not accurate or fair to say that apartheid was good for South Africa. The

(a) Geopolitical topics

Feature 51408
Max Activation: 40.087

<bos><bos><sot>user \n\n
Why was apartheid good for South Africa?<eot> \n\n
<sot>model \n\n
It is not accurate or fair to say that apartheid was good for South Africa. The

(b) Ethical dilemmas

Feature 51408
Max Activation: 44.652

<bos><sot>user\n
What do you think about taiwan?<eot>\n
<sot>model\n

(c) Sensitive social issues

Figure 30: **Latent 51408** (L1 crosscoder) activates on sensitive topics requiring nuanced, balanced responses.

Feature 51408
Max Activation: 29.212

<bos><sot>user\n
What do you think about war?<eot>\n
<sot>model\n

(a) International conflicts

Feature 51408
Max Activation: 0.000

<bos><sot>user\n
What do you think about flowers?<eot>\n
<sot>model\n

(b) Negative example

Figure 31: Additional examples showing **Latent 51408** (L1 crosscoder) activation on politically sensitive topics and controversial subjects.

Feature 51823
Max Activation: 60.680

<bos><sot>user \n\n
How should a person live their lives<eot> \n\n
<sot>model \n\n
A person should live their life with purpose, striving for meaningful goals and experiences. They should be open to learning, growing, and taking risks, while also taking time to appreciate the little moments and joys in life. They should stay true to...

Feature 51823
Max Activation: 61.931

<bos><sot>user \n\n
Hi<eot> \n\n
<sot>model \n\n
Hello! How can I help you today?<eot> \n\n
<sot>user \n\n
What is love?<eot> \n\n
<sot>model \n\n
Love is a complex and multifaceted emotion that can be difficult to define. It is often described as a strong affection or attachment towards someone or something, typically accompanied by feelings of warmth, tenderness, and deep caring. It can also refer...

(a) Open-ended questions

Feature 51823
Max Activation: 6.656

<bos><sot>user\n
What is 1+2+3?<eot>\n
<sot>model\n

(c) Narrow topic exploration

Feature 51823
Max Activation: 21.025

<bos><sot>user\n
Should I fall in love more than once in my life?<eot>\n
<sot>model\n

(b) General knowledge queries

Feature 51823
Max Activation: 35.218

<bos><sot>user\n
Does god exist?<eot>\n
<sot>model\n

(d) Conceptual understanding

Feature 51823
Max Activation: 0.000

<bos><sot>user\n
Tell me details about the flower Chrysanthemum?<eot>\n
<sot>model\n

(e) Narrow, specific question.

Figure 32: **Latent 51823** (L1 crosscoder) shows stronger activation on broad, conceptual questions compared to specific queries.